Circulation Research
JOURNAL OF THE AMERICAN HEART ASSOCIATION

Smooth Muscle Cells Differentiated From Reprogrammed Embryonic Lung Fibroblasts Through DKK3 Signaling Are Potent for Tissue Engineering of Vascular GraftsNovelty and Significance

Eirini Karamariti, Andriana Margariti, Bernhard Winkler, Xiaocong Wang, Xuechong Hong, Dilair Baban, Jiannis Ragoussis, Yi Huang, Jing-Dong J. Han, Mei Mei Wong, Can M. Sag, Ajay M. Shah, Yanhua Hu and Qingbo Xu

Circ Res. 2013;112:1433-1443; originally published online March 25, 2013;
doi: 10.1161/CIRCRESAHA.111.300415
Circulation Research is published by the American Heart Association, 7272 Greenville Avenue, Dallas, TX 75231

Print ISSN: 0009-7330. Online ISSN: 1524-4571

Smooth Muscle Cells Differentiated From Reprogrammed Embryonic Lung Fibroblasts Through DKK3 Signaling Are Potent for Tissue Engineering of Vascular Grafts

Eirini Karamariti,* Andriana Margariti,* Bernhard Winkler, Xiaocong Wang, Xuechong Hong, Dilair Baban, Jiannis Ragoussis, Yi Huang, Jing-Dong J. Han, Mei Mei Wong, Can M. Sag, Ajay M. Shah, Yanhua Hu, Qingbo Xu

Rationale: **Smooth muscle cells (SMCs) are a key component of tissue-engineered vessels. However, the sources by which they can be isolated are limited.**

Objective: **We hypothesized that a large number of SMCs could be obtained by direct reprogramming of fibroblasts, that is, direct differentiation of specific cell lineages before the cells reaching the pluripotent state.**

Methods and Results: **We designed a combined protocol of reprogramming and differentiation of human neonatal lung fibroblasts. Four reprogramming factors (OCT4, SOX2, KLF4, and cMYC) were overexpressed in fibroblasts under reprogramming conditions for 4 days with cells defined as partially-induced pluripotent stem (PiPS) cells. PiPS cells did not form tumors in vivo after subcutaneous transplantation in severe combined immunodeficiency mice and differentiated into SMCs when seeded on collagen IV and maintained in differentiation media. PiPS-SMCs expressed a panel of SMC markers at mRNA and protein levels. Furthermore, the gene dickkopf 3 was found to be involved in the mechanism of PiPS-SMC differentiation. It was revealed that dickkopf 3 transcriptionally regulated SM22 by potentiation of Wnt signaling and interaction with Kremen1. Finally, PiPS-SMCs repopulated decellularized vessel grafts and ultimately gave rise to functional tissue-engineered vessels when combined with previously established PiPS-endothelial cells, leading to increased survival of severe combined immunodeficiency mice after transplantation of the vessel as a vascular graft.**

Conclusions: **We developed a protocol to generate SMCs from PiPS cells through a dickkopf 3 signaling pathway, useful for generating tissue-engineered vessels. These findings provide a new insight into the mechanisms of SMC differentiation with vast therapeutic potential. (*Circ Res*. 2013;112:1433-1443.)**

Key Words: animal models ■ smooth muscle cells ■ stem cells ■ vascular progenitors ■ vascular tissue engineering

Vascular tissue engineering has the potential to provide biological substitutes for repair or replacement of damaged or blocked vessels in patients.[1] Recent reports demonstrated that several techniques using different sources of endothelial cells (ECs) and smooth muscle cells (SMCs) were developed to produce small diameter conduits.[1–4] However, the lack of high numbers of autologous vessels for complicated surgeries remains problematic.[4,5] Because SMCs are a major component of vessels and play an important role throughout the vascular system, undeniably they would be expected to improve the functional characteristics of bioengineered vessels.[6] SMCs have been isolated from adult arteries and used for tissue-engineered vessels. These SMCs divide a finite number of times before undergoing growth arrest, a state known as senescence, attributable to progressive telomere erosion that proceeds with each cell division.[7,8] Finding a new cell source that will provide large amounts of SMCs is important for the development of vascular tissue engineering as treatment for vascular diseases. We have previously demonstrated that embryonic stem cells can differentiate into SMCs via different signal pathways.[9–13] However, the initial signals that stimulate the differentiation of embryonic stem cells in vitro and in vivo still remain unclear.

In This Issue, see p 1401
Editorial, see p 1402

Original received October 29, 2012; revision received March 19, 2013; accepted March 25, 2013. In February 2013, the average time from submission to first decision for all original research papers submitted to *Circulation Research* was 11.98 days.

From the Cardiovascular Division, British Heart Foundation Centre, King's College London, UK (E.K., A.M., B.W., X.W., X.H., M.M.W., C.M.S., A.M.S., Y.H., Q.X.); The Wellcome Trust Centre for Human Genetics, University of Oxford, Oxford, UK (D.B., J.R.); and Chinese Academy of Sciences Key Laboratory of Computational Biology, Max Planck Partner Institute for Computational Biology, Shanghai Institutes for Biological Sciences, Shanghai, China (Y.H., J.-D.J.H., H.Y.).

*These authors contributed equally to this work.

The online-only Data Supplement is available with this article at http://circres.ahajournals.org/lookup/suppl/doi:10.1161/CIRCRESAHA.111.300415/-/DC1.

Correspondence to Qingbo Xu, MD, PhD, Cardiovascular Division, King's British Heart Foundation Centre, King's College London, 125 Coldharbour Ln, London SE5 9NU. E-mail qingbo.xu@kcl.ac.uk

Nonstandard Abbreviations and Acronyms	
Ctl	control
DKK3	dickkopf 3
DM	differentiation medium
ECs	endothelial cells
iPS cells	induced pluripotent stem cells
PiPS cells	partially-induced pluripotent stem cells
SCID	severe combined immunodeficiency
SMCs	smooth muscle cells

Somatic cell reprogramming is a stochastic process during which extensive epigenetic modifications and chromatin remodeling takes place to accommodate the activation of pluripotent loci and the inactivation of lineage-specific genes.[14] Studies with inducible vectors have shown that during reprogramming, intermediate populations that can ultimately give rise to induced pluripotent stem (iPS) cells are generated.[15,16] This knowledge combined with the use of transcription factors for induction of pluripotency, led to the hypothesis that accordingly specific combinations of transcription factors and culture conditions could lead to reprogramming from one somatic cell fate to another without an intermediate pluripotent state. Consequently, partially-iPS (PiPS) cells were generated.[17]

Dickkopf 3 (DKK3) is the most divergent member of the dickkopf family, which seems to have a decisive function in myogenic cell fate, because it was recently found to be highly expressed in different skeletal muscle subtypes.[18] Further evidence showing that DKK3 positively regulates the expression of myf5, a transcription factor regulating muscle differentiation, adds to its role in myogenesis.[19] DKK3 could also have an intracellular function because it was recently shown to directly interact with βTrCP (negative regulator of β-catenin).[20] However, the involvement of DKK3 in SMC differentiation from stem/progenitor cells remains unknown. In the present study, the potential of PiPS cells to differentiate into functional SMCs was thoroughly investigated. We demonstrated a method that generates PiPS-SMCs via a DKK3 pathway and provided evidence that PiPS-derived SMCs can be used for the generation of functional tissue-engineered vessels, capable of mimicking native vessels in in vivo animal models.

Methods

Generation of PiPS Cells

PiPS cells were generated as previously described.[17] Briefly, human embryonic lung fibroblasts were nucleofected with a polycistronic plasmid containing all 4 factors (Oct4, Sox2, Klf4, and cMyc; Addgene Plasmid 20866: pCAG2LMKOSimO).[21] They were then maintained in reprogramming media on gelatin for 4 days.[17]

Cell Differentiation

PiPS cells were seeded on collagen IV (5 μg/mL) and maintained in differentiation media (DM). The cells were cultured in DM for 4 days after which they were harvested and further analyzed.

Generation of Tissue-Engineered Vessels and Artery Graft Procedure

PiPS cells or fibroblasts were seeded in decellularized vessels and differentiated to SMCs and ECs for the generation of double-seeded, tissue-engineered vessels. These vessels were then grafted in the carotid artery of severe combined immunodeficiency (SCID) mice for 1 to 3 weeks.

Statistical Analysis

The data were analyzed using Graph Pad Prism Software. The data expressed as the means±SEM were analyzed with a 2-tailed student *t* test for 2 groups. A value of $P<0.05$ was considered significant. Detailed Methods are included in the Online Data Supplement.

Results

Characterization of PiPS Cells

During somatic cell reprogramming extensive molecular changes occur, leading to the differential expression of several genes. Microarray analysis of samples at 4, 7, 14, and 21 days during fibroblast cell reprogramming revealed that the expression levels of a great number of genes were altered from as early as day 4 (Online Figure I and Online Table II). Therefore, PiPS cells were generated and characterized as previously shown.[17] Human fibroblasts were nucleofected with a linearized plasmid encoding all 4 genes and maintained in reprogramming media for 4 days. Simultaneously, fibroblasts, nucleofected with an empty vector, were maintained in reprogramming media and used as controls (ctl). Although PiPS cells did not form colonies at this stage (Figure 1B), they displayed morphological differences when compared with ctl cells (Figure 1A). PiPS cells expressed the 4 genes at the mRNA level (Figure 1C) and expressed kinase insert domain receptor (vascular endothelial growth factor receptor 2), as revealed by fluorescence-activated cell sorting analysis (Figure 1D). Finally, PiPS cells were negative for alkaline phosphatase (Figure 1E–1G) and did not form teratomas in vivo 2 months after subcutaneous transplantation in SCID mice, as shown by hematoxylin/eosin staining (Figure 1H–1M), and immunofluorescence for markers specific for the 3 germ layers (Online Figure II). PiPS cells were labeled with Vybrant to demonstrate successful incorporation within the tissues (Online Figure IV).

PiPS Cells Can Differentiate Into SMCs

We have recently shown that PiPS cells can differentiate into functional ECs in response to vascular endothelial growth factor under specific culture conditions.[17] Hence, in this study, the potential of PiPS cells to differentiate into vascular SMCs was assessed. PiPS cells were seeded on collagen IV and maintained in DM, based on a previously established SMC differentiation protocol.[9] After 4 days of differentiation, PiPS cells exhibited a SMC-like morphology (Figure 2B) comparable to primary SMCs (Figure 2C) as opposed to the ctl population where cells maintained their fibroblast morphology (Figure 2A). Furthermore, they expressed SMC-specific markers in a time-dependent manner at the mRNA level (Figure 2D and 2E). More specifically, on day 4, the differentiated PiPS cells expressed a full panel of SMC-specific markers at the mRNA level (Figure 2F) and smooth muscle actin, calponin, and SM22 at the protein level (Figure 2G). Additionally, immunofluorescence for calponin and SM22 demonstrated a SMC-like morphology when compared with ctl cells (Figure 2H), with an efficiency of 42.5% for calponin and 38% for

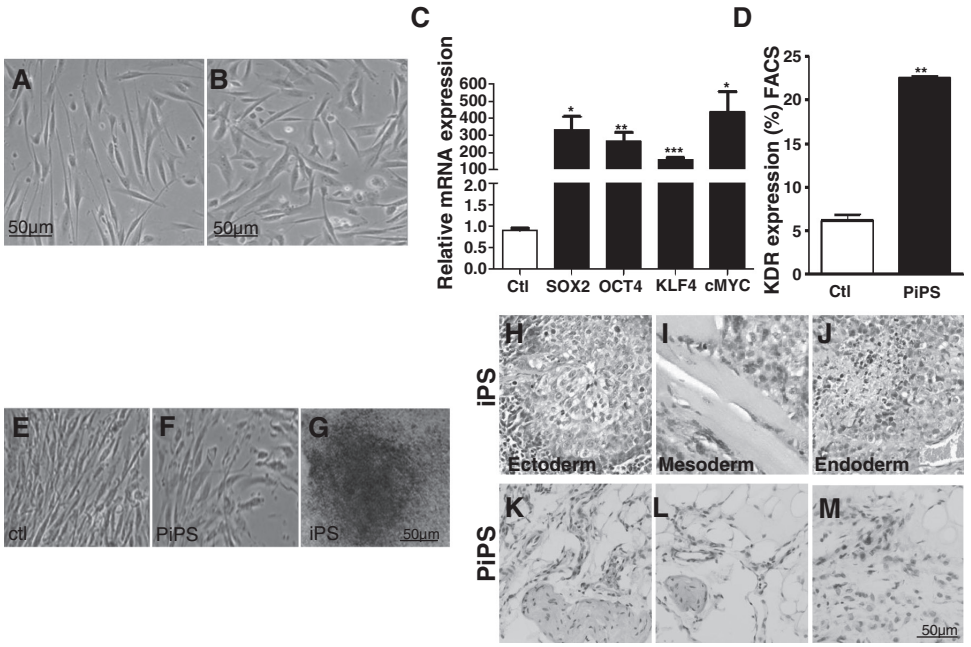

Figure 1. Characterization of partially-induced pluripotent stem (PiPS) cells. Human embryonic fibroblasts were nucleofected with pCAG2LMKOSimO (PiPS cells) or empty vectors (control [ctl] cells) and maintained in reprogramming conditions for 4 days as previously described. Morphological differences between ctl (**A**) and PiPS cells (**B**) are apparent after 4 days of reprogramming. PiPS cells express the 4 reprogramming factors SOX2, OCT4, KLF4, and cMYC at the mRNA level (**C**) as revealed by quantitative real-time polymerase chain reaction (mean±SEM of n=3; **P*<0.05; ***P*<0.01; ****P*<0.001). Fluorescence-activated cell sorting (FACS) analysis revealed an increased expression of kinase insert domain receptor (KDR, vascular endothelial growth factor receptor 2) in PiPS cells when compared with the ctl cells (**D**; mean±SEM of n=3; ***P*<0.01). PiPS cells were negative for the embryonic stem cell marker alkaline phosphatase (**E**–**G**) and did not proceed to teratoma formation after 2 months of in vivo transplantation in severe combined immunodeficiency mice as revealed by hematoxylin/eosin staining (**K**–**M**), contrary to the induced pluripotent stem (iPS) cells (**H**–**J**).

SM22 (Figure 2I). Moreover, PiPS-SMCs showed elevated levels of elastin and collagen IA1, which are characteristic of large artery SMCs (Figure 2J). Interestingly, selection of PiPS cells with neomycin during reprogramming revealed a 100% efficiency of differentiation to SM22-positive cells, whereas the nonreprogrammed cells remained in a fibroblastic state (Online Figure V). Finally, fluorescence-activated cell sorting analysis for the proliferation marker Ki67 revealed an almost identical proliferation rate between PiPS-SMCs and human SMCs (Figure 2K), whereas stimulation of PiPS-SMCs with 60 mmol/L KCl caused them to contract as shown in Online Movie I in a way similar to human SMCs (Online Movie II). It should be noted that investigation of additional lineage markers revealed that this protocol is specific for SMC generation (Online Figure VI). Collectively, these results demonstrate that PiPS cells can differentiate to functional SMCs, which were defined as PiPS-SMCs.

DKK3 Is Involved in the Differentiation of PiPS Cells to SMCs

When elucidating the mechanism of PiPS-SMC differentiation, a member of the dickkopf family, DKK3, was identified from the microarray analysis to be correlated to the reprogramming process toward SMCs. DKK3 was upregulated in parallel with SMC markers during PiPS-SMC differentiation at both the mRNA (Figure 3A) and protein levels (Figure 3B). Furthermore, immunofluorescence confirmed the concomitant expression of DKK3 with SMC-specific markers, revealing a stronger perinuclear pattern of DKK3 in the differentiated PiPS-SMCs when compared with the ctl cells (Figure 3C and 3D). Additionally, DKK3 was transiently overexpressed in PiPS-SMC during differentiation. Upregulation of DKK3 led to further induction of SMC-specific markers at the protein level (Figure 3E and 3F). These results suggest that DKK3 is involved in PiPS-SMC differentiation. To address whether DKK3 is sufficient to drive PiPS-SMC differentiation, the aforementioned gene was suppressed via lentiviral delivery of short hairpin DKK3 during differentiation. SMC-specific markers were downregulated at the mRNA level (Figure 3G) concomitant to the downregulation of DKK3. Interestingly, further investigation of cardiovascular lineage markers after DKK3 overexpression or knockdown did not reveal any significant expression changes, suggesting that the effect of DKK3 is SMC-specific (Online Figure VIII). These results show that DKK3 is essential for PiPS-SMC differentiation.

Cytokine Role of DKK3 in PiPS-SMC Differentiation

DKK3 is a secreted glycoprotein expressed in a variety of tissues, and its role as a cytokine has previously been reported.[22] However, its physiological role remains unclear. To investigate the role of DKK3 as a cytokine in PiPS-SMC differentiation, the supernatant of 4-day differentiated PiPS and ctl cells was collected. DKK3 ELISA measurements revealed that there was an increased release of DKK3 in the supernatant of PiPS-SMCs when compared with that of ctl cells (Figure 4A). To ascertain whether DKK3 has a cytokine effect in our system, a human recombinant DKK3 cytokine was used to stimulate PiPS-SMCs. PiPS cells were differentiated for 3 days and then stimulated with human recombinant DKK3 for

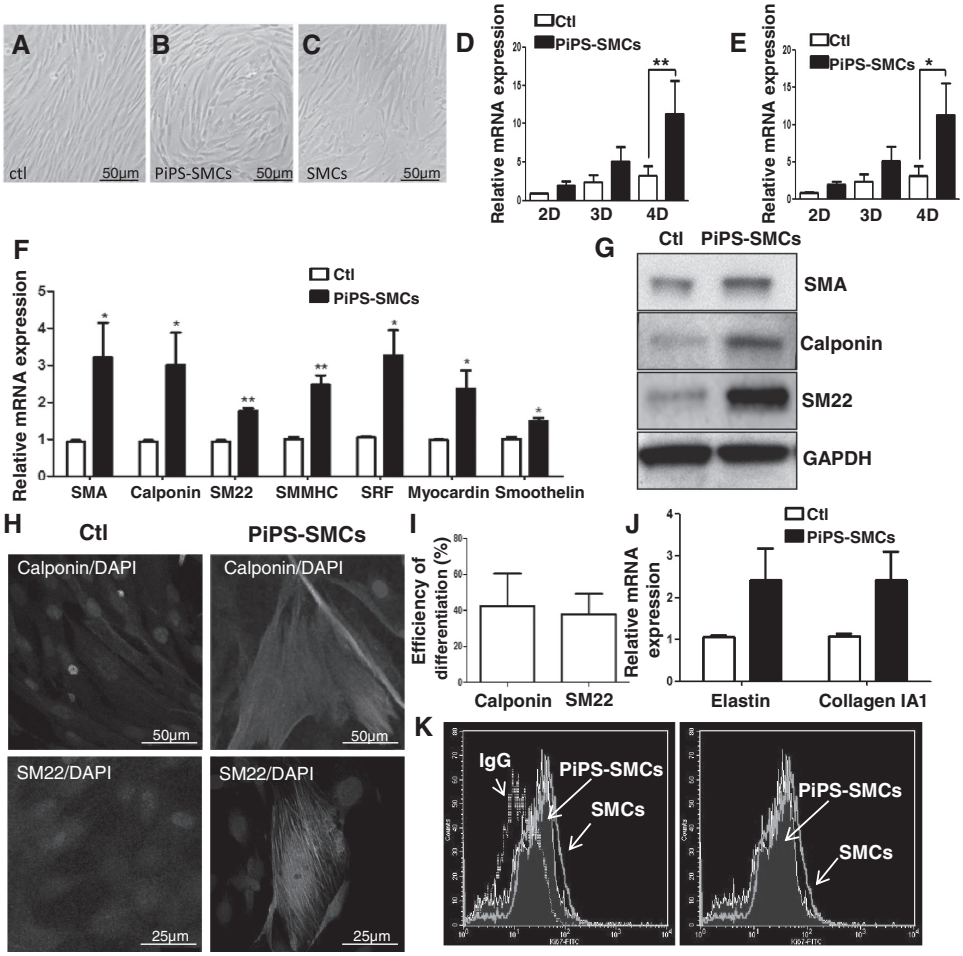

Figure 2. Partially-induced pluripotent stem (PiPS) cells can differentiate to smooth muscle cells (SMCs). PiPS cells or control (ctl) cells were seeded on collagen IV and maintained in differentiation media for 4 days. Contrary to ctl cells (**A**), PiPS-SMCs (**B**) have adopted a SMC-like morphology as comparable with native SMCs (**C**) and expressed SMC-specific markers, such as smooth muscle actin (SMA; **D**) and calponin (**E**), on a time-dependent manner (mean±SEM of n=3; **P*<0.05; ***P*<0.01). More specifically, on day 4, PiPS-SMCs expressed a full panel of SMC markers at the mRNA level (**F**) and the SMC markers, SMA, calponin, and SM22 at the protein level (**G**). Immunofluorescent staining showed a typical SMC staining for calponin and SM22 as revealed by confocal microscopy (**H**) and quantitative immunofluorescence revealed an efficiency of 42.5% for calponin and 38% for SM22 positive cells (**I**). Quantitative real-time polymerase chain reaction analysis for elastin and collagen I A1 revealed an upregulation in PiPS-SMCs when compared with the ctl cells (**J**; mean±SEM of n=3; **P*<0.05; ***P*<0.01). FACS analysis for the proliferation marker Ki67 revealed similar proliferation patterns between SMCs and PiPS-SMCs (**K**). SRF indicates serum response factor.

24 hours. Analysis of the samples revealed an upregulation of SMC specific marker expression at both the mRNA and protein levels between stimulated and unstimulated PiPS-SMCs, as shown by quantitative real-time polymerase chain reaction (Figure 4B) and Western blot (Figure 4C and 4D), respectively. These results suggest that DKK3 secretion plays an important role in PiPS-SMC differentiation.

DKK3 Regulates the Transcriptional Activation of SM22 Through Activation of Wnt Signaling

To clarify the molecular mechanism regulated by DKK3 during PiPS-SMCs differentiation, the effect of DKK3 in the transcriptional activation of SMC-specific markers was evaluated. Luciferase assays were performed, and the promoter activity of SM22 was detected. PiPS cells during SMC differentiation were cotransfected with a reporter gene pGL3-Luc-SM22 vector[23] and a plasmid encoding DKK3. The results revealed that there was an upregulation of the SM22 promoter activity on DKK3 overexpression (Figure 5A), suggesting that DKK3 induced the activation of SM22 at the transcriptional level. To further confirm the effect of DKK3, the promoter activity of SM22 was also detected after knockdown by short hairpin DKK3, revealing a decrease in the transcriptional activation of SM22 (Figure 5B). These results confirmed the effect of DKK3 in the transcriptional regulation of SM22 during PiPS-SMC differentiation. It has previously been shown that β-catenin, the downstream mediator of Wnt signaling, directly regulates the transcription of SM22 by binding to its −213 to −192 upstream promoter region.[24] In our PiPS-SMCs differentiation model, an increased level of β-catenin expression was detected in PiPS-SMCs when compared with the ctl cells at both the mRNA (Figure 5C) and protein levels (Figure 5D and 5E). Furthermore, DKK3 as part of the dickkopf family of Wnt inhibitors has been implicated in activation or deactivation of Wnt signaling, although its role remains unclear.[25,26] Therefore, to test whether DKK3 induced

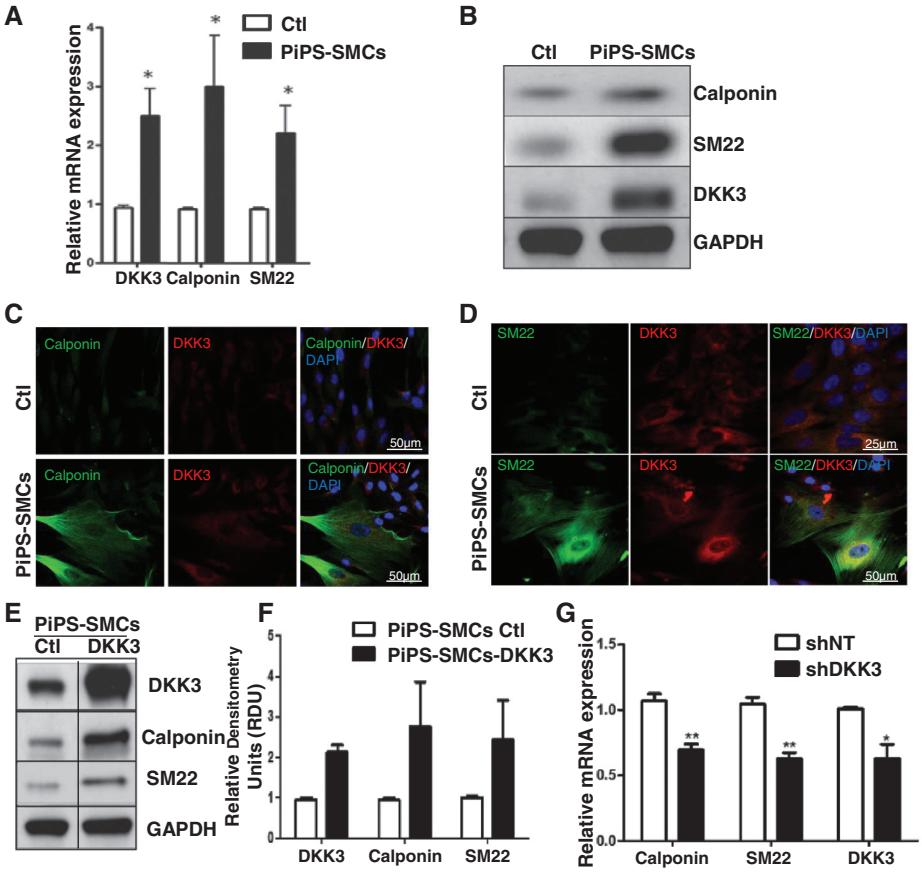

Figure 3. Dickkopf 3 (DKK3) is involved in partially-induced pluripotent stem-smooth muscle cell (PiPS-SMC) differentiation. DKK3 expression was upregulated in parallel with SMC-specific markers on day 4 of differentiation in PiPS-SMCs at both the mRNA and protein levels as revealed by quantitative real-time polymerase chain reaction (**A**; mean±SEM of n=3; **P*<0.05) and Western blot analysis, (**B**) respectively. Immunofluorescent staining revealed a concomitant expression of DKK3 and the SMC markers, calponin and SM22, in PiPS-SMCs, with DKK3 appearing in a perinuclear pattern (**C** and **D**). DKK3 overexpression with a DKK3 plasmid or a pCMV5 empty vector in PiPS-SMCs at 2 days revealed a further induction of SMC markers at the protein level (**E** and **F**) when assessed on day 4. DKK3 was knocked down with shDKK3 in PiPS-SMCs at day 1 of differentiation, showing a suppression of SMC markers on day 4 at the mRNA level (**G**; mean±SEM of n=3; **P*<0.05; ***P*<0.01).

PiPS cell differentiation to SMCs through its interaction with the Wnt signaling pathway, the activation status of Wnt was initially assessed. A TopFlash vector (transcription factor reporter plasmid) was used to measure the promoter activity of the Wnt signaling target genes on DKK3 overexpression in differentiating PiPS cells. Detection of the luciferase activity revealed an upregulation in the reporter activity of TopFlash reporter genes during induction of DKK3 (Figure 5F). Investigation of the transcriptional patterns of the Wnt pathway targets β-catenin, transcription factor 1 and Axin2

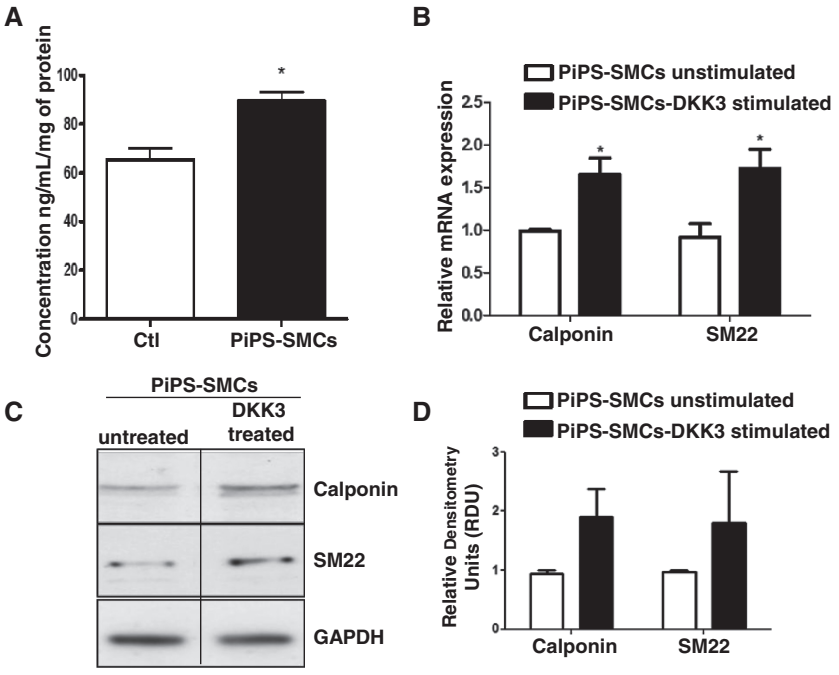

Figure 4. The cytokine role of dickkopf 3 (DKK3) in partially-induced pluripotent stem-smooth muscle cell (PiPS-SMC) differentiation. Supernatant from PiPS-SMCs and control (ctl) cells was collected at day 4 of differentiation and subjected to a DKK3 ELISA assay (**A**). It was revealed that there is an increased release of DKK3 in the supernatant of PiPS-SMCs when compared with the ctl cells (mean±SEM of n=3; **P*<0.05). Stimulation of PiPS-SMCs with 50 ng/mL of human recombinant DKK3 cytokine in serum-free media for 24 hours revealed a further upregulation of SMC markers at the mRNA and protein levels as revealed by quantitative real-time polymerase chain reaction (**B**; mean±SEM of n=3; **P*<0.05) and Western blot (**C** and **D**).

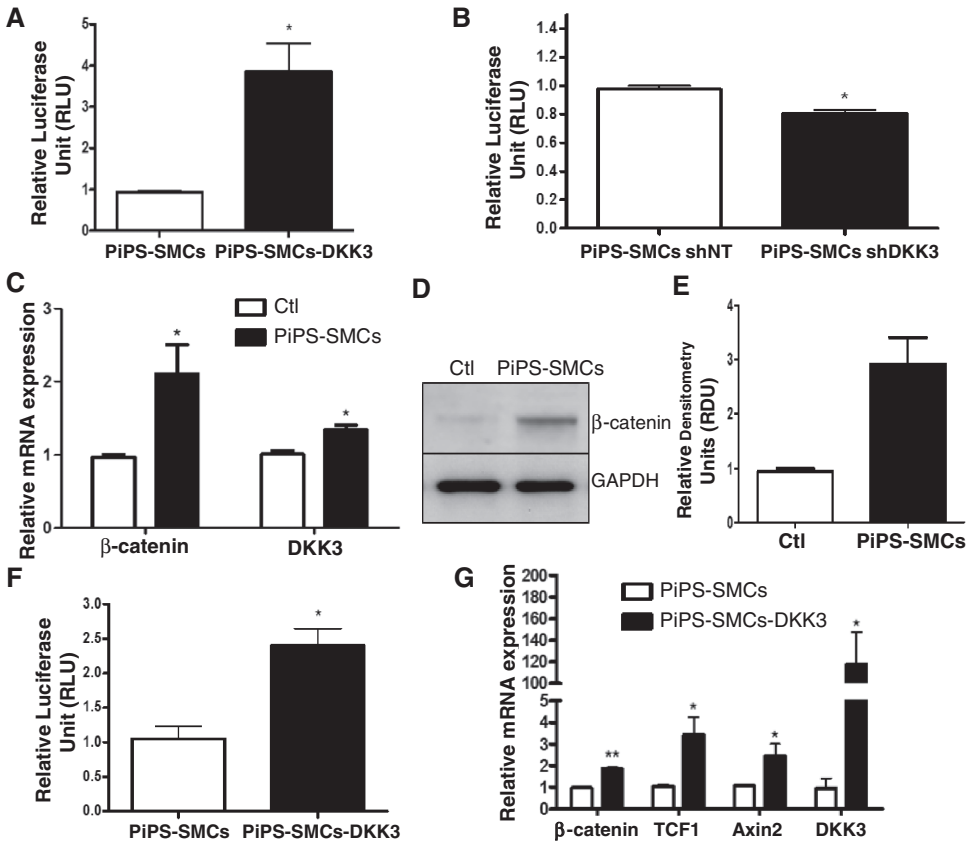

Figure 5. Dickkopf 3 (DKK3) regulates the transcriptional activation of SM22 through activation of Wnt signaling. Luciferase assays were performed in cells overexpressing DKK3 or an empty pCMV5 vector at day 4 of differentiation (**A**). It was revealed that there is an increased promoter activity for SM22 in the presence of DKK3 (mean±SEM of n=3; **P*<0.05). Luciferase assays were also performed in cells, where DKK3 was silenced by shDKK3 at day 4 of partially-induced pluripotent stem-smooth muscle cell (PiPS-SMC) differentiation (**B**), where it was found that there is a decreased promoter activity for SM22. Quantitative real-time polymerase chain reaction (q-PCR) results (**C**; mean±SEM of n=3; **P*<0.05) and Western blot analysis (**D** and **E**) show an increased expression of β-catenin in PiPS-SMCs when compared with the control (ctl) cells. Luciferase assays in cells overexpressing DKK3 or an empty pCMV5 vector at day 4 (**F**) revealed an increased promoter activity for TopFlash in the presence of DKK3, suggesting Wnt signaling activation (mean±SEM of n=3; **P*<0.05). q-PCR revealed a further upregulation of β catenin after overexpression of DKK3 in PiPS-SMCs, as well as an increase of the Wnt signaling targets transcription factor (TCF) 1 and Axin2 at the mRNA level (**G**; mean±SEM of n=3; **P*<0.05; ***P*<0.01).

in PiPS-SMC-DKK3 cells revealed an upregulation in the expression of these targets (Figure 5G). Interestingly, further investigation into the expression of a number of Wnt elements in both PiPS-SMCs and PiPS-SMC-DKK3 cells did not reveal any significant changes in the expressions of LRPs, SFRPs, and DKKs but revealed an upregulation of Wnts and the Frizzled receptor 1 (Online Figure IX).These findings further support the notion that upregulation of DKK3 leads to activation of Wnt signaling during PiPS-SMC differentiation.

DKK3 Regulates PiPS-SMC Differentiation Through β-catenin Nuclear Translocation

It has previously been shown that after inhibition of the β-catenin destruction complex, the cytoplasmic β-catenin, is stabilized and can enter the nucleus to interact with the transcription factor/lymphoid enhancer-binding factor family of transcription factors, promoting specific gene expression.[27] Therefore, we postulated whether DKK3 could induce the translocation of β-catenin into the nucleus and subsequently the transcriptional regulation of SM22 and the Wnt signaling target genes. Indeed, immunofluorescent staining showed that β-catenin was translocated into the cell nucleus on DKK3 stimulation in PiPS-SMCs (Figure 6A). To confirm that the DKK3-induced regulation of SM22 is mediated by β-catenin, the reporter activity of the SM22 promoter was assessed after silencing of β-catenin in PiPS-SMCs (Figure 6B) and in PiPS-SMC-DKK3 cells with simultaneous knockdown of β-catenin (Figure 6C). Interestingly, shβ-catenin leads to a dramatic downregulation of the SM22 promoter activity in PiPS-SMCs, whereas knockdown of β-catenin in PiPS-SMC-DKK3 cells leads to a downregulation of the SM22 promoter activity negating the effect of DKK3. Additionally, luciferase assays for the activation of the SM22 promoter after overexpression of DKK3 that were performed after mutation of the Wnt-responsive element (–213 to –192) within the promoter revealed the attenuation of the DKK3 effect on the SM22 promoter activation (Figure 6E). Collectively, these results demonstrate that the transcriptional activation of SM22 by DKK3 is mediated by β-catenin nuclear translocation.

DKK3 Activates Wnt Signaling Through Interaction With Kringle Containing Transmembrane Protein 1

Thus far, our data have demonstrated that transcriptional activation of SM22 by DKK3 was mediated by β-catenin.

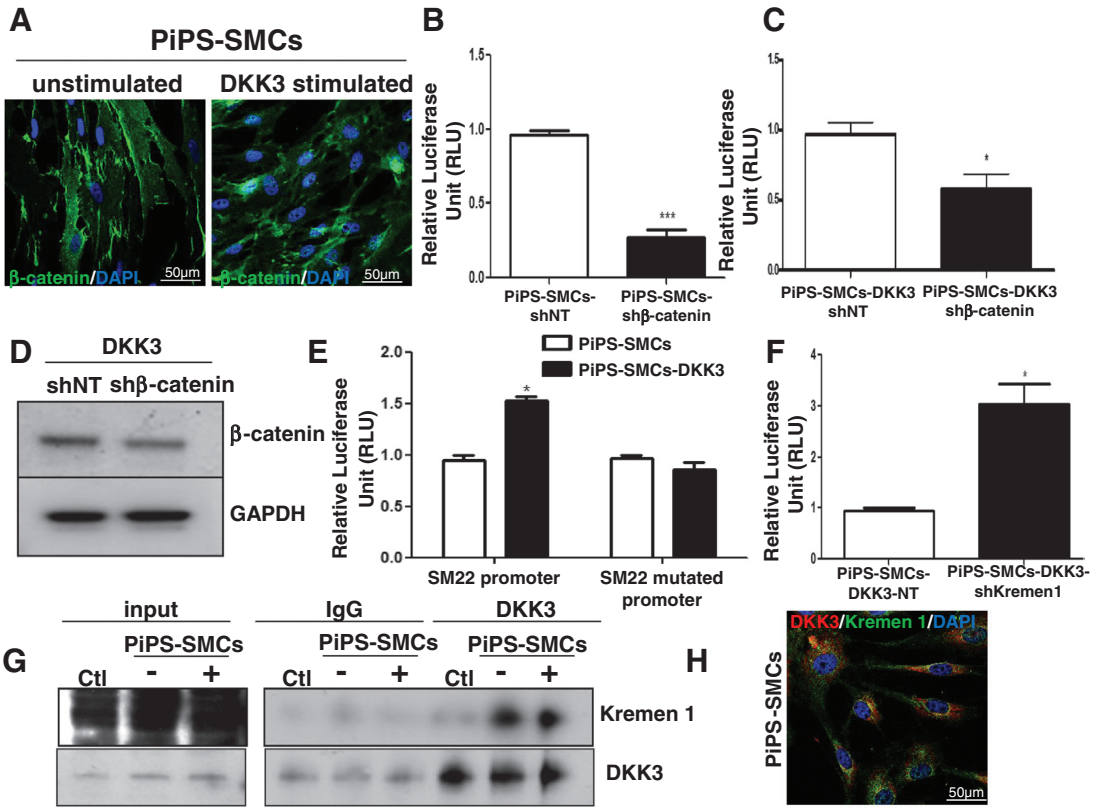

Figure 6. Activation of Wnt signaling through β-catenin translocation and binding of dickkopf 3 (DKK3) on Kringle containing transmembrane protein 1 (Kremen1). Partially-induced pluripotent stem-smooth muscle cell (PiPS-SMC) were stimulated for 6 hours with 50 ng/mL human recombinant DKK3 cytokine in serum-free and cytokine-free conditions. Immunofluorescent staining revealed the translocation of β-catenin in the nucleus of PiPS-SMCs on 6 hours of DKK3 stimulation (**A**). Luciferase assays performed in PiPS cells after β-catenin knockdown revealed a significant downregulation of the SM22 promoter activity (**B**; mean±SEM of n=3; ***P<0.001). Additionally, luciferase assays were performed in PiPS-SMC-DKK3 cells, whereas β-catenin was silenced by shβ-catenin (**C**). It was revealed that the upregulation of SM22 promoter activity in the presence of DKK3 is ablated on knockdown of β-catenin (mean±SEM of n=3; *P<0.05). Downregulation of β-catenin was confirmed by Western blot analysis (**D**). Luciferase assays for activation of the SM22 promoter after overexpression of DKK3 were also performed after mutation of the Wnt-responsive element within the promoter. The DKK3-induced activation of SM22 is attenuated after mutation of the −213 to −192 upstream promoter region (**E**; mean±SEM of n=3; *P<0.05). Luciferase assays for TopFlash activity were also performed in PiPS-SMCs overexpressing DKK3, whereas Kremen1 was knocked down. The results revealed an even further induction of Wnt signaling after the combined effect of DKK3 induction and Kremen1 knockdown (**F**; mean±SEM of n=3; *P<0.05). Control (ctl), PiPS-SMCs, and PiPS-SMCs stimulated with 50 ng/mL human recombinant DKK3 cytokine were subjected to immunoprecipitation with rabbit DKK3. Western blot analysis of the precipitated complexes (**G**) revealed binding of DKK3 with Kremen1 in PiPS-SMCs and stimulated PiPS-SMCs when compared with the ctl cells. Indirect immunofluorescent experiments in PiPS-SMCs revealed a colocalization of Kremen1 and DKK3 in a perinuclear pattern (**H**).

To elucidate the underlying mechanism of this regulation, the interaction of DKK3 with proteins of the Wnt signaling pathway was assessed. It has recently been reported that DKK3 can potentiate Wnt signaling through interaction with the kringle containing transmembrane protein 1 (Kremen1).[28] Thus, we questioned whether the activation of Wnt in our system is mediated through interaction of DKK3 with Kremen1. Whole cell lysates from ctl cells, PiPS-SMCs, and PiPS-SMCs stimulated with 50 ng/mL human recombinant DKK3 were subjected to immunoprecipitation using DKK3. Subsequent immunoblotting with Kremen1 showed that although no binding between DKK3 and Kremen1 was revealed in the ctl cells, the aforementioned proteins show strong binding in PiPS-SMCs and PiPS-SMC-DKK3-stimulated cells (Figure 6G). To further confirm this interaction, double immunofluorescent staining for DKK3 and Kremen1 was performed, which revealed a clear colocalization of the 2 proteins in a distinct perinuclear pattern (Figure 6H). Finally, to confirm the function of Kremen1 in association to Wnt signaling, luciferase assays for TopFlash, in PiPS-SMC-DKK3 cells where Kremen1 was silenced by shKremen1, were performed revealing further induction of Wnt activation after concomitant Kremen1 knockdown and DKK3 induction (Figure 6F). These findings postulate that the response of PiPS-SMCs to DKK3 and the subsequent activation of Wnt signaling occurs though binding of DKK3 to Kremen1.

PiPS-SMCs Display SMC Properties Ex Vivo and In Vivo

To test the functionality of the PiPS-SMCs, an ex vivo model generated in our laboratory was used. Fibroblasts or PiPS cells selected with neomycin were seeded on a decellularized vessel scaffold in a specially constructed bioreactor in DM suspension containing 25 ng/mL platelet-derived growth factor-BB. Both vessels were harvested 5 days later. The ex vivo PiPS-SMC vessels stained positive for several SMC markers

and exhibited the characteristic morphology and localization of SMCs in the media of the vessels. Such staining was not obtained by the fibroblast-derived vessels (Online Figure XI).

In addition, the functionality of PiPS-SMCs and PiPS-ECs, as well as their potential to generate patent vessels comparable with native vessels, was investigated. A population of PiPS cells after selection with neomycin was seeded on a decellularized vessel in DM containing 25 ng/mL platelet-derived growth factor-BB, where it was initially differentiated toward SMCs for 48 hours. The circulating medium was then exchanged to endothelial growth media 2 (EGM-2 as endothelial specific medium) and a second seeding step of selected PiPS cells was performed. The vessels remained under constant shear stress for 5 days after which they were harvested. Hematoxylin/eosin staining of normal mouse vessels, decellularized vessels, as well as the ex vivo double-seeded vessels, revealed that their recellularization with PiPS-SMCs and PiPS-ECs resulted to vessels that greatly resembled a native mouse artery (Figure 7A–7C). Furthermore, double immunofluorescence revealed characteristic staining for the EC-specific markers, CD31 and CD144, and SMC markers, smooth muscle actin and SM22, as well as characteristic localization of PiPS-SMCs and PiPS-ECs, within the vessel scaffold (Figure 7D–7I). Subsequently, to assess the patency of the tissue-engineered vessels in in vivo conditions, normal mouse arteries, decellularized arteries, and the PiPS cell-derived vessels were grafted into mice (Online Movie III). It was revealed that the mice engrafted with the decellularized vessels presented with high mortality rates from as early as day 1, whereas the mice that received the double-seeded, tissue-engineered vascular grafts presented with a survival rate of 60%, 3 weeks after transplantation (Figure 8). Additional in vivo studies revealed that although transplantation of decellularized vessel grafts leads to rupture and transplantation of fibroblast-derived vessel grafts leads to occlusion of the vessel, transplantation of the double-seeded, tissue-engineered grafts leads to the generation of patent vessels mimicking healthy native vessels (Online Figure XII). Furthermore, the 3-week-old grafts were fully characterized in terms of the presence of human PiPS-SMCs, ECs, and host macrophage infiltration (Online Figures XIII and XIV). These results indicate that PiPS cells are capable of differentiating into both vascular lineages and are potent for generating functional tissue-engineered vessels, capable of substituting native vessels in vivo.

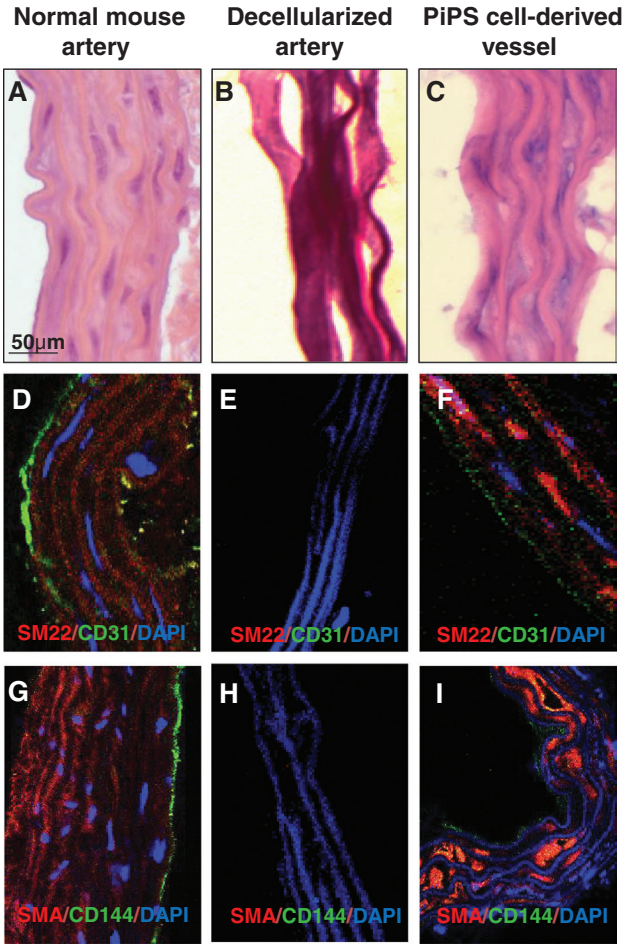

Figure 7. Generation of double-seeded, tissue-engineered vascular grafts. Partially-induced pluripotent stem-smooth muscle cell (PiPS-SMC) and PiPS-endothelial cells (Ecs) display SMC and EC properties, respectively, as well as recellularization properties in tissue-engineered vessels. Hematoxylin/eosin (HE) staining of the double-seeded vessels (**C**) revealed an architecture similar to that of native vessels (**A**) with multiple layers of SMCs and a monolayer of ECs. Successful decellularization is confirmed by the absence of cells in the HE-stained decellularized vessel (**B**). Double-seeded, tissue-engineered vessels (**F** and **I**) stained positive for EC and SMC markers. The concomitant expression of SMC and EC markers, as well as the characteristic morphology and localization of PiPS-SMCs and PiPS-ECs, within the media and intima was comparable to that of native vessels (**D** and **G**). SMA indicates smooth muscle actin.

Discussion

Vascular SMCs play a critical role in both the physiological maintenance of the cardiovascular system and the pathophysiology of vascular diseases in adults.[29,30] They are also a major component in engineered vascular grafts, particularly, in the generation of large vessels. In the present study, we used a shortcut method to successfully reprogram fibroblasts to functional SMCs, that is, PiPS-SMCs. PiPS-SMC differentiation was found to be regulated by a DKK3 signaling pathway. As demonstrated by our ex vivo experiments, PiPS-SMCs form vascular structures when seeded in a specially constructed bioreactor and differentiated into mature SMC phenotypes. Importantly, when engrafted into SCID mice, the aforementioned tissue-engineered vessels displayed a function in vivo. Therefore, it can be concluded that the strategy used here for the first time to generate PiPS-SMCs is a fast, simple, efficient, and reproducible method for obtaining SMCs, which could constitute a valuable tool for regenerative medicine, cell replacement therapy, as well as tissue engineering.

The accumulating knowledge concerning the use of transcription factor–based reprogramming enhanced the idea of direct lineage reprogramming circumventing pluripotency. In agreement with previous studies,[31,32] our microarray analysis results reveal that the expression patterns of genes associated with fundamental processes of the cell, such as differentiation and cell growth, are altered from as early as day 4 during reprogramming. We have recently shown that 4-day reprogrammed cells termed PiPS cells

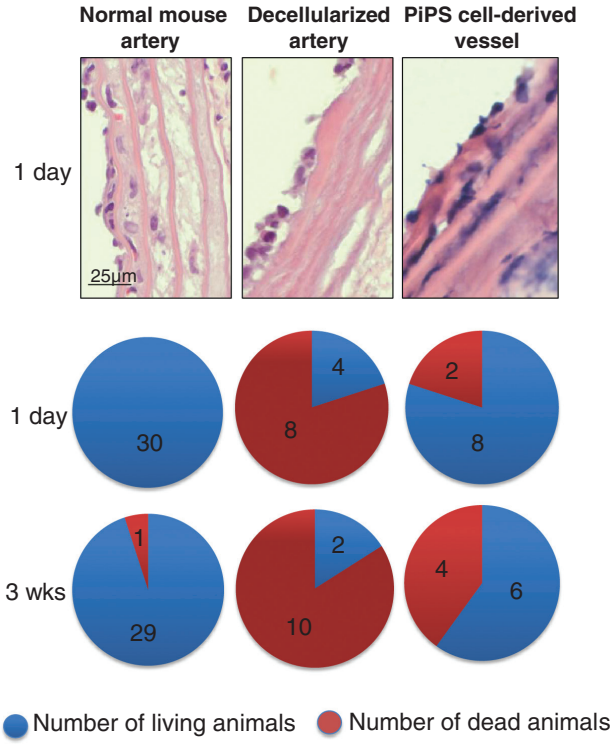

Figure 8. Partially-induced pluripotent stem (PiPS) cell–derived, tissue-engineered vascular grafts are patent for substituting native vessels in vivo. Normal mouse artery, decellularized artery, and PiPS cell–derived vessels were engrafted in the carotid artery of severe combined immunodeficiency mice. The mice engrafted with the PiPS cell–derived grafts presented with a 60% survival rate 3 weeks after surgery, whereas the survival rate of mice engrafted with decellularized arteries was significantly lower (20%; n=10).

can differentiate into functional ECs in response to defined media and culture conditions. PiPS cells did not form tumors after subcutaneous transplantation in SCID mice rendering them safe for clinical applications.[17] Further configuration of the identity of PiPS cells did not reveal significant changes in the expression of ectodermal or endodermal markers (Online Figure III). However, PiPS cells expressed kinase insert domain receptor, the first molecule to be expressed during development with specificity to the endothelium,[33] suggesting that a vascular program has already initiated after 4 days of reprogramming.[17] Thus in the present study, the potential of PiPS cells to differentiate to SMC was investigated, and PiPS-SMCs were successfully generated and characterized. Interestingly, selection of PiPS cells for the kinase insert domain receptor revealed a higher upregulation of SM22 and myocardin (data not shown), which in conjunction to the lack of upregulation of ectodermal markers in PiPS cells suggests a mesodermal origin of PiPS-SMCs within our system of differentiation. Notably, PiPS cells, generated from adult skin fibroblasts and differentiated as previously described, did not reveal significant SMC marker upregulations at day 4. This suggests that further optimization of the differentiation protocol, such as increase of the Oct-Sox-Klf-Myc transfection efficiency or longer differentiation time points, are imperative for direct differentiation of more mature cell lines to SMCs.

The generation of PiPS-SMCs has several implications. Initially, the time from reprogramming to obtaining SMC is significantly shorter when compared with the time-consuming generation of iPS cells and redifferentiation to the desired cell line. This offers the opportunity to generate patient-specific cells quickly and efficiently for personalized cell therapy. Additionally, one of the main concerns of stem cell and iPS cell therapy, which is tumorigenesis, is eliminated. Moreover, they are generated by using a nonintegrative method of overexpression of the 4 reprogramming factors and, if required, they can be selected to obtain populations of high purity, thus making them a more accessible and reliable source of cells for use in regenerative medicine.

Elucidation of the mechanism of PiPS-SMC differentiation revealed the involvement of DKK3, a gene whose expression was altered during the initial stages of reprogramming. DKK3 has mainly been implicated in cancer disease.[34–36] Recently, DKK3 was associated with tumor angiogenesis and was considered a putative proangiogenic factor and marker for neo angiogenesis,[37] as well as a differentiation factor involved in remodeling of the tumor vasculature.[38] In the present study, it is shown that DKK3 can regulate the transcriptional patterns of SM22 via promoter activation. It is also demonstrated that DKK3 can act as a cytokine and that it can positively modulate the canonical Wnt signaling and induce β-catenin translocation and ultimately induction of Wnt target genes. Importantly, this potentiating effect of DKK3 within our system seems to be unique because DKK1 was found to negatively regulate Wnt signaling in PiPS-SMCs in accordance with previously published data[39] (Online Figure X). Finally, we demonstrated that DKK3 interacts with the transmembrane protein Kremen1. Our results showed that PiPS-SMC differentiation was induced through a DKK3-Wnt signaling pathway, giving DKK3 a novel function with possible developmental and therapeutic implications (Online Figure XVIII).

Short-term reprogramming could reinforce the expression of important cell fate–determining genes, which regulate several differentiation pathways and make cells amenable to responding to specific stimulus.[40] Interestingly, application of lineage-specific differentiation in PiPS cells showed that their differentiation potential may not be limited to vascular cell lineages. Preliminary studies show that PiPS cells can respond to defined culture conditions for neuronal, adipocyte, chondrocyte, and osteocyte differentiation and can express markers specific for these lineages on differentiation (Online Figure XIX). It would, therefore, be interesting to investigate the multipotent potential of PiPS cells.

After the generation of the first in vitro blood vessel more than 30 years ago, this particular research area has seen considerable progress in terms of scaffold availability, construction of the vessels, and application of stem cells.[1] Studies have shown that decellularized vessels treated with heparin alone can successfully be applied in animal models; however, it is widely accepted that this approach would not be applicable in humans and that multilayers of SMCs, as well as an endothelial layer in the vessel wall, are essential for the prevention of graft rupture and atherosclerosis.[2] In the present study, we developed a method to seed decellularized vessel scaffolds with PiPS cells on both the adventitial and

luminal sides. Using this method, an artery-like vessel was created containing several layers of SMCs between the elastic lamina and a monolayer of ECs investing the inner surface of the vessel. Importantly, the PiPS tissue-engineered vessels are mostly patent, whereas the majority of decellularized grafts presented with occlusion or ruptured within 24 hours of grafting into SCID mice. Failure of some tissue-engineered vessels over time could be the result of inflammatory responses caused by macrophages. Nevertheless, the major advantage of these tissue-engineered vessels is primarily the source of the cells used. PiPS cells are capable of differentiating into both ECs and SMCs making the technique of generating the grafts in ex vivo conditions less complicated and significantly faster. Additionally, transplantation of PiPS or fibroblasts in vivo does not lead to tumorigenesis. Interestingly, ex vivo contractility assays of the tissue-engineered vessels revealed that although the cells can successfully contract within the decellularized scaffold, tension bath contraction assays may not be suitable for assessing the functionality of the generated vessels (Online Figures XV and XVI). Thus, the present study provides a method of generating tissue-engineered vessels ex vivo, as well as a suitable mouse model, for assessing the function of the generated vessel grafts.

Summarizing, we have established a method to generate PiPS cells using human fibroblasts, which can effectively differentiate into SMCs via a DKK3 signaling pathway. PiPS cells can incorporate in decellularized vessel scaffolds by differentiating into both ECs and SMCs, leading to the generation of patent tissue-engineered vessels capable of mimicking native vessels when engrafted into an animal model. Although direct reprogramming between lineages is currently in its infancy, usage of the current knowledge and the continuous effort to expand our basic understanding of somatic cell reprogramming can revolutionize the field of regenerative medicine and make patient-specific therapy a reality in the near future.

Sources of Funding

This work was supported by the British Heart Foundation and the Oak Foundation.

Disclosures

None.

References

1. L'Heureux N, Dusserre N, Marini A, Garrido S, de la Fuente L, McAllister T. Technology insight: the evolution of tissue-engineered vascular grafts–from research to clinical practice. *Nat Clin Pract Cardiovasc Med*. 2007;4:389–395.
2. Zhang WJ, Liu W, Cui L, Cao Y. Tissue engineering of blood vessel. *J Cell Mol Med*. 2007;11:945–957.
3. O'Cearbhaill ED, Punchard MA, Murphy M, Barry FP, McHugh PE, Barron V. Response of mesenchymal stem cells to the biomechanical environment of the endothelium on a flexible tubular silicone substrate. *Biomaterials*. 2008;29:1610–1619.
4. Gong Z, Niklason LE. Small-diameter human vessel wall engineered from bone marrow-derived mesenchymal stem cells (hMSCs). *FASEB J*. 2008;22:1635–1648.
5. Kaushal S, Amiel GE, Guleserian KJ, Shapira OM, Perry T, Sutherland FW, Rabkin E, Moran AM, Schoen FJ, Atala A, Soker S, Bischoff J, Mayer JE Jr. Functional small-diameter neovessels created using endothelial progenitor cells expanded ex vivo. *Nat Med*. 2001;7:1035–1040.
6. Xiao Q, Wang G, Luo Z, Xu Q. The mechanism of stem cell differentiation into smooth muscle cells. *Thromb Haemost*. 2010;104:440–448.
7. Bierman EL. The effect of donor age on the in vitro life span of cultured human arterial smooth-muscle cells. *In Vitro*. 1978;14:951–955.
8. Bonin LR, Madden K, Shera K, Ihle J, Matthews C, Aziz S, Perez-Reyes N, McDougall JK, Conroy SC. Generation and characterization of human smooth muscle cell lines derived from atherosclerotic plaque. *Arterioscler Thromb Vasc Biol*. 1999;19:575–587.
9. Xiao Q, Zeng L, Zhang Z, Hu Y, Xu Q. Stem cell-derived Sca-1+ progenitors differentiate into smooth muscle cells, which is mediated by collagen IV-integrin alpha1/beta1/alphav and PDGF receptor pathways. *Am J Physiol Cell Physiol*. 2007;292:C342–C352.
10. Xiao Q, Luo Z, Pepe AE, Margariti A, Zeng L, Xu Q. Embryonic stem cell differentiation into smooth muscle cells is mediated by Nox4-produced H2O2. *Am J Physiol Cell Physiol*. 2009;296:C711–C723.
11. Zhang L, Jin M, Margariti A, Wang G, Luo Z, Zampetaki A, Zeng L, Ye S, Zhu J, Xiao Q. Sp1-dependent activation of HDAC7 is required for platelet-derived growth factor-BB-induced smooth muscle cell differentiation from stem cells. *J Biol Chem*. 2010;285:38463–38472.
12. Pepe AE, Xiao Q, Zampetaki A, Zhang Z, Kobayashi A, Hu Y, Xu Q. Crucial role of Nrf3 in smooth muscle cell differentiation from stem cells. *Circ Res*. 2010;106:870–879.
13. Xiao Q, Pepe AE, Wang G, Luo Z, Zhang L, Zeng L, Zhang Z, Hu Y, Ye S, Xu Q. Nrf3-Pla2g7 interaction plays an essential role in smooth muscle differentiation from stem cells. *Arterioscler Thromb Vasc Biol*. 2012;32:730–744.
14. Mikkelsen TS, Hanna J, Zhang X, Ku M, Wernig M, Schorderet P, Bernstein BE, Jaenisch R, Lander ES, Meissner A. Dissecting direct reprogramming through integrative genomic analysis. *Nature*. 2008;454:49–55.
15. Stadtfeld M, Maherali N, Breault DT, Hochedlinger K. Defining molecular cornerstones during fibroblast to iPS cell reprogramming in mouse. *Cell Stem Cell*. 2008;2:230–240.
16. Hanna J, Saha K, Pando B, van Zon J, Lengner CJ, Creyghton MP, van Oudenaarden A, Jaenisch R. Direct cell reprogramming is a stochastic process amenable to acceleration. *Nature*. 2009;462:595–601.
17. Margariti A, Winkler B, Karamariti E, Zampetaki A, Tsai TN, Baban D, Ragoussis J, Huang Y, Han JD, Zeng L, Hu Y, Xu Q. Direct reprogramming of fibroblasts into endothelial cells capable of angiogenesis and reendothelialization in tissue-engineered vessels. *Proc Natl Acad Sci USA*. 2012;109:13793–13798.
18. de Wilde J, Hulshof MF, Boekschoten MV, de Groot P, Smit E, Mariman EC. The embryonic genes Dkk3, Hoxd8, Hoxd9 and Tbx1 identify muscle types in a diet-independent and fiber-type unrelated way. *BMC Genomics*. 2010;11:176.
19. Hsu RJ, Lin CC, Su YF, Tsai HJ. Dickkopf-3-related gene regulates the expression of zebrafish Myf5 gene through phosphorylated p38a-dependent Smad4 activity. *J Biol Chem*. 2011;286:6855–6864.
20. Lee EJ, Jo M, Rho SB, Park K, Yoo YN, Park J, Chae M, Zhang W, Lee JH. Dkk3, downregulated in cervical cancer, functions as a negative regulator of beta-catenin. *Int J Cancer*. 2009;124:287–297.
21. Kaji K, Norrby K, Paca A, Mileikovsky M, Mohseni P, Woltjen K. Virus-free induction of pluripotency and subsequent excision of reprogramming factors. *Nature*. 2009;458:771–775.
22. Watanabe M, Kashiwakura Y, Huang P, Ochiai K, Futami J, Li SA, Takaoka M, Nasu Y, Sakaguchi M, Huh NH, Kumon H. Immunological aspects of REIC/Dkk-3 in monocyte differentiation and tumor regression. *Int J Oncol*. 2009;34:657–663.
23. Margariti A, Xiao Q, Zampetaki A, Zhang Z, Li H, Martin D, Hu Y, Zeng L, Xu Q. Splicing of HDAC7 modulates the SRF-myocardin complex during stem-cell differentiation towards smooth muscle cells. *J Cell Sci*. 2009;122:460–470.
24. Shafer SL, Towler DA. Transcriptional regulation of SM22alpha by Wnt3a: convergence with TGFbeta(1)/Smad signaling at a novel regulatory element. *J Mol Cell Cardiol*. 2009;46:621–635.
25. Nakamura RE, Hunter DD, Yi H, Brunken WJ, Hackam AS. Identification of two novel activities of the Wnt signaling regulator Dickkopf 3 and characterization of its expression in the mouse retina. *BMC Cell Biol*. 2007;8:52.
26. Yue W, Sun Q, Dacic S, Landreneau RJ, Siegfried JM, Yu J, Zhang L. Downregulation of Dkk3 activates beta-catenin/TCF-4 signaling in lung cancer. *Carcinogenesis*. 2008;29:84–92.
27. Novak A, Dedhar S. Signaling through beta-catenin and Lef/Tcf. *Cell Mol Life Sci*. 1999;56:523–537.
28. Nakamura RE, Hackam AS. Analysis of Dickkopf3 interactions with Wnt signaling receptors. *Growth Factors*. 2010;28:232–242.

29. Campbell JH, Campbell GR. The role of smooth muscle cells in atherosclerosis. *Curr Opin Lipidol*. 1994;5:323–330.
30. Owens GK. Regulation of differentiation of vascular smooth muscle cells. *Physiol Rev*. 1995;75:487–517.
31. Yuan X, Wan H, Zhao X, Zhu S, Zhou Q, Ding S. Brief report: combined chemical treatment enables Oct4-induced reprogramming from mouse embryonic fibroblasts. *Stem Cells*. 2011;29:549–553.
32. Efe JA, Hilcove S, Kim J, Zhou H, Ouyang K, Wang G, Chen J, Ding S. Conversion of mouse fibroblasts into cardiomyocytes using a direct reprogramming strategy. *Nat Cell Biol*. 2011;13:215–222.
33. Carmeliet P, Ferreira V, Breier G, et al. Abnormal blood vessel development and lethality in embryos lacking a single VEGF allele. *Nature*. 1996;380:435–439.
34. Tsuji T, Miyazaki M, Sakaguchi M, Inoue Y, Namba M. A REIC gene shows down-regulation in human immortalized cells and human tumor-derived cell lines. *Biochem Biophys Res Commun*. 2000;268:20–24.
35. Hoang BH, Kubo T, Healey JH, Yang R, Nathan SS, Kolb EA, Mazza B, Meyers PA, Gorlick R. Dickkopf 3 inhibits invasion and motility of Saos-2 osteosarcoma cells by modulating the Wnt-beta-catenin pathway. *Cancer Res*. 2004;64:2734–2739.
36. Kobayashi K, Ouchida M, Tsuji T, Hanafusa H, Miyazaki M, Namba M, Shimizu N, Shimizu K. Reduced expression of the REIC/Dkk-3 gene by promoter-hypermethylation in human tumor cells. *Gene*. 2002;282:151–158.
37. Zitt M, Untergasser G, Amberger A, Moser P, Stadlmann S, Zitt M, Müller HM, Mühlmann G, Perathoner A, Margreiter R, Gunsilius E, Ofner D. Dickkopf-3 as a new potential marker for neoangiogenesis in colorectal cancer: expression in cancer tissue and adjacent non-cancerous tissue. *Dis Markers*. 2008;24:101–109.
38. Fong D, Hermann M, Untergasser G, Pirkebner D, Draxl A, Heitz M, Moser P, Margreiter R, Hengster P, Amberger A. Dkk-3 expression in the tumor endothelium: a novel prognostic marker of pancreatic adenocarcinomas. *Cancer Sci*. 2009;100:1414–1420.
39. Mao B, Wu W, Davidson G, Marhold J, Li M, Mechler BM, Delius H, Hoppe D, Stannek P, Walter C, Glinka A, Niehrs C. Kremen proteins are Dickkopf receptors that regulate Wnt/beta-catenin signalling. *Nature*. 2002;417:664–667.
40. Ieda M, Fu JD, Delgado-Olguin P, Vedantham V, Hayashi Y, Bruneau BG, Srivastava D. Direct reprogramming of fibroblasts into functional cardiomyocytes by defined factors. *Cell*. 2010;142:375–386.

Novelty and Significance

What Is Known?

- The sources of obtaining smooth muscle cells (SMCs) for the generation of tissue-engineered vessels are scarce.
- SMCs could be directly reprogrammed from one lineage to another.

What New Information Does This Article Contribute?

- Fibroblasts subjected to short-term reprogramming can successfully differentiate into SMCs termed partially-induced pluripotent stem (PiPS)-SMCs.
- PiPS-SMCs can contribute to the generation of functional tissue-engineered vessels, which can mimic native mouse vessels when engrafted into an animal model.

SMCs constitute a large part of the vessel wall, which makes them an important component of tissue-engineered vascular grafts. However, the sources by which they are isolated are limited, and de novo generation of SMCs from pluripotent cells can be challenging because of inefficient and time-consuming protocols. Herein, we report that we have successfully differentiated semireprogrammed fibroblasts termed PiPS cells into functional SMCs. In addition, we have identified Dickkopf 3 as novel SMC differentiation regulator and have elucidated the signaling pathway by which Dickkopf 3 regulates PiPS-SMCs differentiation. Furthermore, using PiPS-SMCs, we have generated tissue-engineered vascular grafts that when engrafted into a mouse model will function like native vessels. These findings add to the current knowledge of direct reprogramming between lineages providing an ample source of functional SMCs for use in tissue engineering. Moreover, we have identified a simple and fast method for generating tissue-engineered vascular grafts as well as a suitable mouse model for testing the functionality of these vessels in vivo.

SUPPLEMENTAL MATERIAL

Materials and Methods

Antibodies: mouse anti-SMA (Sigma, A5228), mouse anti-SMA-Cy3™ (Sigma, C6198), rabbit anti-calponin (abcam, ab46794), rabbit anti-SM22 (abcam, 14106), goat anti-DKK3 (R&D, AF1118), rabbit β-catenin (Santa Cruz, sc-7199), rabbit anti-GAPDH (Santa Cruz, Sc-25778), goat anti-Kremen 1 (R&D, AF1647). Mouse anti-human Nestin, mouse anti-Neuron-specific β-III Tubulin, mouse anti-Oligodendrocyte Marker O4, rat anti-Fibroblast Marker (ER-TR7)(Santa Cruz, sc-52353), goat anti-mouse FABP-4 (962643), mouse anti-human Osteocalcin (962645), goat anti-human Aggrecan (962644), and anti-hVEGF (R2/KDR, FAB357F), anti-human CD31 were from R&D Systems. Rabbit anti-CD144 (cell signalling, 2158), rat monoclonal against mouse MAC-1 (PharMingen, San Diego, CA). The secondary antibodies anti-goat Alexa488, anti-goat Alexa594, anti-rabbit Alexa488 and anti-rabbit Alexa594 were purchased from Invitrogen.

Microarray analysis. Fibroblasts were infected with 4 lentiviral vectors (EX-Z0092-v08-OCT4, EX-Z2845-Lv08-v-Myc, EX-Q0453-Lv08-KLF4, EXT2547-Lv08-SOX2) purchased from GeneCopoeia. An empty vector (Ex-Lv08) was used as control. Samples were collected at timpeoints 4, 7, 14 and 21 days, RNA was extracted and a microarray analysis was performed and compared to control groups[1].

Cell culture. Prenatal human embryonic lung fibroblasts from ATCC (CCL-153™) were cultured on gelatin (0.04% of 2% Solution Type B from Bovine Skin, Sigma G1393) in ATCC F-12K Medium (ATCC, 30-2004) supplemented with 10% ATCC Fetal Bovine Serum (ATCC, 30-2020) and 100 U/mL penicillin/streptomycin in a humidified incubator with 5% CO_2. Cells were passaged every 3 days in a ratio of 1:3 or 1:7 and the medium was refreshed every 2 days.

Umbilical Artery SMCs purchased from Lonza (Cat. No cc-2579 Lot 7F3804) were maintained in the SMC specific media SmGM-2 BulletKit (Cat No. CC-3181 & CC-4149) and were used as positive controls for FACS and contractility assays.

Human adult dermal fibroblasts were also purchased form Lonza (Cat. No cc-2511 Lot 0000247101) and were maintained in specific media FBM Fibroblast Basal (Cat. No. cc-3131). The cells were passages in a ratio of 1:3 to 1:6 and the medium was refreshed every 2 days.

PiPS labelling. PiPS cells were labelled with Molecular Probes Vybrant Cell Labelling (MP22885) before they were subcutaneously injected into SCID mice as part of the teratoma formation experiment.

PiPS selection. Human neonatal fibroblasts were nucleofected with the polycistronic OSKM plasmid containing all four factors as previously described[2]. Neomycin selection (Sigma G418, Cat. No. G8168) at a concentration of 25 μg/ml was initiated 24 hours after the nucleofection and continued up to day 4 when a pure population of PiPS cells expressing the mOrange fluorescent marker as well as the four transcription factors was obtained.

Cell differentiation. PiPS cells were seeded on collagen IV coated dishes (5μg/ml) and maintained in DM which contained MEM α (Life technologies Cat. No. A10490-01) supplemented with 10% FBS (PAA Cat. No A15-151), 100U/ml penicillin and streptomycin (Life technologies Cat. No. 15070-063), 0.2 mM L-glutamine (Life technologies Cat. No.

25030-024), 0.1mM β-mercaptoethanol (Life technologies Cat. No. 31350-010) and 10ng/ml Platelet Derived Growth Factor BB (PDGF-BB) (R&D systems Cat No: 220-BB). The cells were maintained under these conditions for 4 days after which they were harvested and further analysed.

Contractility assay. PiPS-SMCs and UASMCs were seeded in 6 well plates in low densities. They were then stimulated with 60mM KCl and visualised over a period of 45 minutes with timelapse phase contrast microscopy which resulted in the movies S1 and S2.

FACS analysis. PiPS or control cells and isotype controls were analysed with FACS in order to test the percentage of the KDR positive cells. Furthermore, PiPS-SMCs or UASMCs and isotype controls were analysed in Data analysis was carried out using CellQuest software (Becton Dickinson).

Enzyme-linked immunosorbent assay (ELISA). The concentration of the DKK3 released glycoprotein in the supernatant was detected by an R&D DKK3 ELISA kit (R&D, DY1118) according to the protocol provided.

Treatment with human recombinant DKK3 cytokine. PiPS cells were seeded on collagen IV for differentiation into SMCs for 2 days. The medium was refreshed with serum free medium in which the cells were maintained overnight. The following day they were stimulated with 50ng/ml human recombinant DKK3 cytokine (R&D, 1118DK) overnight or for 6 hours for the β-catenin translocation and co-immunoprecipitation experiments.

Reverse transcriptase-polymerase chain reaction (RT-PCR) and Q-PCR

RT-PCR and Real-Time PCR was performed as previously described[3]. Total RNA was extracted using the RNeasy Mini Kit (Qiagen) according to the manufacturer's protocol. Conventional PCR primers were designed using the Primer-BLAST tool (www.ncbi.nlm.gov.uk/tools/primer-blast) whereas Q-PCR primers were designed using a software provided by DNA Integrated Technologies (IDT) (http://eu.idtdna.com/scitools/Applications/RealTimePCR/). The primer sequences are shown in Table S1.

Indirect immunofluorescent staining.

The procedure used for immunofluorescent staining was similar to that previously described[3]. Briefly, cells were fixed with 4% paraformaldehyde, permeabilized with 0.1% Triton X-100 in PBS for 10 min and blocked in 5% swine serum in PBS for 30 min at room temperature. They were then incubated with primary antibodies. The bound primary antibodies were revealed by incubation with the secondary antibodies for 30 minutes at 37^{o}C. Cells were counterstained with 4',6-diamidino-2-phenylindole (DAPI; Sigma), mounted in Floromount-G (Cytomation; DAKO, Glostrup, Denmark), and examined with a fluorescence microscope (Axioplan 2 imaging; Zeiss) or SP5 confocal microscope (Leica, Germany).

Immunoblotting. The method used was similar to that previously described[4]. In short, 25-50μg of protein were boiled in 1xSDS loading buffer for 10 minutes before loading onto NuPage®, 4-12% Bis-Tris gel immersed in NuPage® MOPS SDS running buffer in an XCell SureLock™ Mini-Cell (Life technologies (Novex®) Cat. No. NP0335BOX). The gel was then transferred onto a PVDF membrane (Amersham, hypond-P) with the XCell™ Blot Module (Invitrogen) at 30V for 2 hours and 30 minutes immersed in transfer buffer. The membrane was then blocked with 5% milk in PBS-Tween containing 0.02% sodium azide for

1 hour at room temperature and then incubated in the primary antibody solutions overnight at 4°C.

Fluorescence-activated cell sorting (FACS) analysis. PiPS cells or control (ctl) cells were analysed with FACS in order to test the percentage of the KDR^+ cells as previously described[2]. Data analysis was carried out using CellQuest software (Becton Dickinson). PiPS-SMCs and human SMCs were also analysed for the proliferation marker Ki67 (eBioscience, 11-5698)

Lentiviral particle transduction.

Lentiviral particles were produced using shRNA DKK3 plasmids (ShRNA HSH007526-Lvu6, GeneCopoeia) according to protocol provided and as previously described[4]. The shRNA Non-Targeting (NT) vector was used as a negative control. The supernatant containing the lentivirus was harvested 48h after tranfection, filtered, aliquoted and stored at –80°C. p24 antigen ELISA (Zeptometrix) was used to determine the viral titre. The Transducing Unit (TU) was calculated using the conversion factor recommended by the manufacturer (10^4 physical particles per pg of p24 and 1 transducing unit per 10^3 physical particles for a VSV-G pseudotyped lentiviral vector), with 1pg of p24 antigen converted to 10 Transducing Units (TU). For lentiviral infection, PiPS-SMCs were seeded overnight and the following day were incubated with shDKK3 or shNT as a control ($1x10^7$TU/ml) in complete medium supplemented with 10μg/ml of Polybrene for 24h. Subsequently, fresh medium was added to the cells and the plates were returned to the incubator and harvested 72h later to be subjected to further analysis.

Luciferase activity assay

A pGL3-Luc-SM22[3] and TopFlash vector (Milipore, Cat. No. 21-170) (0.33μg/well) together with the DKK3 expression vector (Addgene: 15496, pCS2-hDKK3-Flag[5]) (0.16μg/well) or the DKK1 expression vector (Addgene: 15494, pCS2-hDKK1-flag[5]) were transiently transfected using FuGene®6 reagent (Promega, Cat. No. E2691) as instructed by the manufacturer. pGL3-Luc-Renilla (0.1μg/ well) was also included in all transfections as an internal control and a pCMV5 vector was used as a mock control. The Luciferase (Luciferase Assay System, Promega, Cat. No. E1501) and Renilla (Coelenterazine, Promega, Cat. No. S200A) enzymatic activities were detected 48 hours after transfection using the Lumat LB 9507 illuminometer. Relative Luciferase Unit (RLU) was defined as the ratio of luciferase activity to Renilla activity with that of control set as 1.0. For experiments where shDKK3 and shβ-catenin were utilised, the cells were seeded until attached, infected with shDKK3, shβ-catenin or shNT and 24 hours later transfected with the promoter, Renilla and control vectors as described above.

SM22 promoter mutation

A luciferase carrying construct were the region between -213 and -192 of the SM22 promoter region was deleted, was generated as previously described[3]. The sequences of the primers used for this mutation can be found in Online Table I.

Co-immunoprecipitation. PiPS cells or ctl cells were seeded on collagen IV coated T75 flasks where they were differentiated for 3 days. The medium of the 3 day differentiated PiPS-SMCs was refreshed to serum free medium overnight. The following day a portion of the serum starved cells were stimulated with 50ng/ml human recombinant DKK3 for 6 hours and subsequently all the samples were harvested and lysed by 1 hour rotation at 4^{o}C. 0.2-1mg of whole cell lysate were subjected to a standard co-immunoprecipitation procedure as previously described[3]. Rabbit anti-DKK3 (Santa Cruz, sc-25518) (0.2 to 1µg) or rabbit IgG were used for complex precipitation and goat anti-Kremen 1 (R&D AF1647) was used as the primary antibody during immunoblotting after reduction of the samples on a NuPage®, 4-12% Bis-Tris gel.

Cell seeding and vascular bioreactor. PiPS cells or fibroblasts were seeded on decellularised aortic grafts (with sodium dodecyl sulfate (SDS) at 0.075 % and washed in PBS) and placed in a specially constructed bioreactor after which sheer stress was applied. Briefly, a roller pump (Masterflex: Standard Drive, model 7520; Standard Pump Head, model 7018-20; Codane Tubing, Cole-Parmer UK) was used to produce mean flow in the bioreactor and the grafts were fixed between two 25 G needles after hosting them on plastic tubes fixed by 8-0 silk sutures (8-0 black virgin silk, Ethicon Inc., Johnson & Johnson, Norderstedt, Germany). The complete setup was maintained in a standard CO_2 incubator at 37°C. The scaffolds were placed for the seeding process in a self-constructed incubation chamber and preconditioned with culture media for 2 hours. 2 x 10^5 PiPS cells or fibroblasts in DM containing 25ng/ml PDGF-BB were seeded on the scaffolds via direct injection and allowed to seed for 12 hours before the initial flow was set up. Decellularised vessels have also been used as a second control. Shear stress was applied at stepwise rates ranging from 5 to 20 dynes/cm^2 over a period of 48 hours. After this time point no increase in the shear stress rate was conducted and the grafts remained under constant shear stress of 20 dynes/cm^2 until they were harvested by day 5. For the last 24 hours 100 U/ml heparin of total circulating reactor media volume (heparin sodium salt diluted, from porcine gastrointestinal mucosa, Sigma Aldrich) was added every 12 hours. For the double seeded PiPS-cell tissue engineered vessels, decellularised vessel scaffolds were placed in a self-constructed incubation chamber and preconditioned with DM containing 25ng/ml PDGF-BB for 2 hours. After this period 2 x 10^6 PiPS cells in DM/PDGF-BB were directly injected and allowed to seed for 12 hours at a continuous rotational movement before initial flow was set up. Shear stress was applied at 10 dynes/cm^2 over a period of 48 hours. Then, the circulating media was exchanged to EGM-2 media[1] and a second seeding step was initiated with 1 x 10^6 PiPS cells. After an additional 12 hour seeding period, the shear stress rate was stepwise adjusted up to 35 dynes/cm^2. The grafts remained under constant shear stress of 35 dynes/cm^2 and harvested on day 5.The engineered vessels were then used for further analysis *ex vivo* or immediately grafted to animals.

Mice and artery graft procedure. All animal experiments were performed according to protocols approved by the Institutional Committee for Use and Care of Laboratory Animals. Tissue engineered vessels were grafted into the carotid artery of NOD.CB17-*Prkdc*^{scid}/NcrCrl mice (Charles River, UK). The vessel graft procedure was similar to that described previously[6]. Briefly, the right common carotid artery was mobilized free from the bifurcation

at the distal end toward the proximal, cut in the middle and a cuff was placed at each end. The artery was turned inside out over the cuff and ligated. The tissue-engineered vessels from the bioreactor were grafted between the two ends of the carotid artery by sleeving the ends of the vessel over the artery cuff and ligating (Movie S3). 24 hours or 3 weeks later, the recipient mice were sacrificed and the grafts were harvested for formalin-fixed sections. The sections were stained with hematoxylin/eosin (HE) and images were assessed by a Zeiss Axioplan 2 Imaging microscope and Axiovision software and processed by Adobe Photoshop software. Magnification was indicated in figure legends as scale bars.

Miller's elastin staining. To assess the elastic lamina in the tissue-engineered vessel sections, the Miller's elastin staining was performed. In brief, paraffin sections were deparaffinised and rehydrated. They were then immersed in potassium permanganate, then in oxalic acid and finally rinsed in 70% ethanol. The tissue was incubated in Miller's elastin dye (BDH Laboratory Supplies, Poole UK) for 3 hours followed by counterstaining with van Gieson solution (50% saturated picric acid solution, 0.09% acid fuchsin) for 5 min. Sections were subsequently dried, dehydrated and mounted on microscope slides. Staining was visualized as described above.

Tension bath contractility assay for tissue engineered vessels. Double seeded tissue engineered vessels were generated like previously described. Decellularised vessels and mouse native vessels were used as negative and positive controls respectively. The native vessels were taken from wild type mice, cleaned from fat and flushed from blood. Native and tissue engineered aortas were then cut into 3mm rings, suspended in Krebs buffer comprising (in mM) NaCl 118.2, KCl 4.69, MgSO47H2O 1.18, KH2PO4 1.19, glucose 11.1, NaHCO3 25.0, CaCl26H2O 2.5 at physiological conditions (pH 7.4 at 37 ^{0}C) and hung into an organ bath system which measures vessel tension under specific stimulation as previously described[7]. Resting tension was set to 2-3g and maintained for at least 30min until steady-state conditions were achieved. The rings were then treated with KCL and PE as shown in Online Figures 15 and 16.

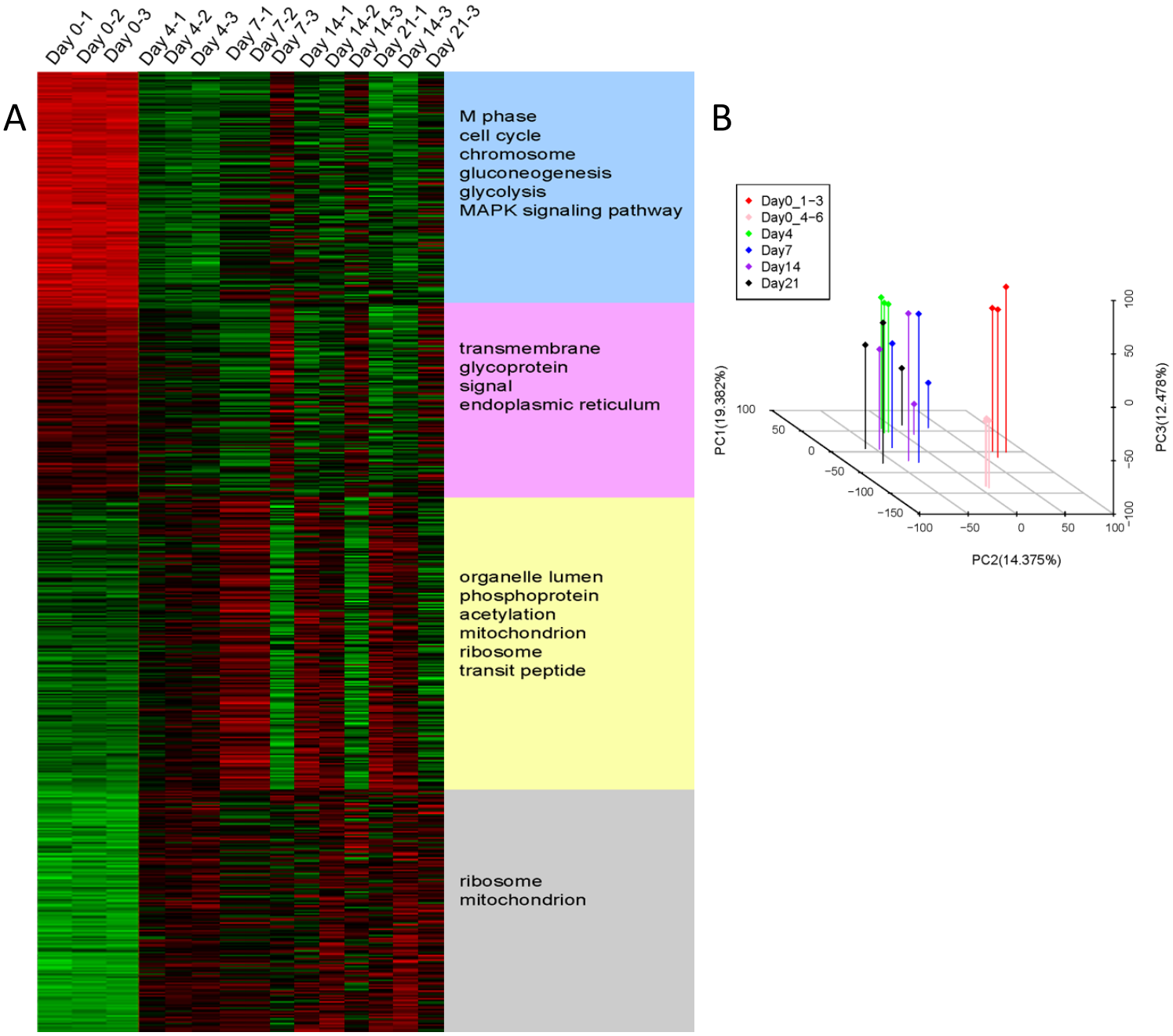

Online Figure I. Microarray analysis of different timepoints during the reprogramming. (A and B) Human fibroblasts were infected with the four factors and maintained in reprogramming conditions for 4, 7, 14 and 21 days. The samples were then subjected to a microarray analysis. Super K-means clustering of the genes whose expressions were correlated to Principle component analysis (PCA) PC2 (|PCC| > 0.5). The biological functions overrepresented in each cluster were determined using the DAVID software. The microarray analysis shows an increased number of genes with altered expression patterns from as early as day 4 when compared to the ctl cells. Furthermore, these genes were associated to fundamental functions of the cell such as cell cycle, metabolism and differentiation.

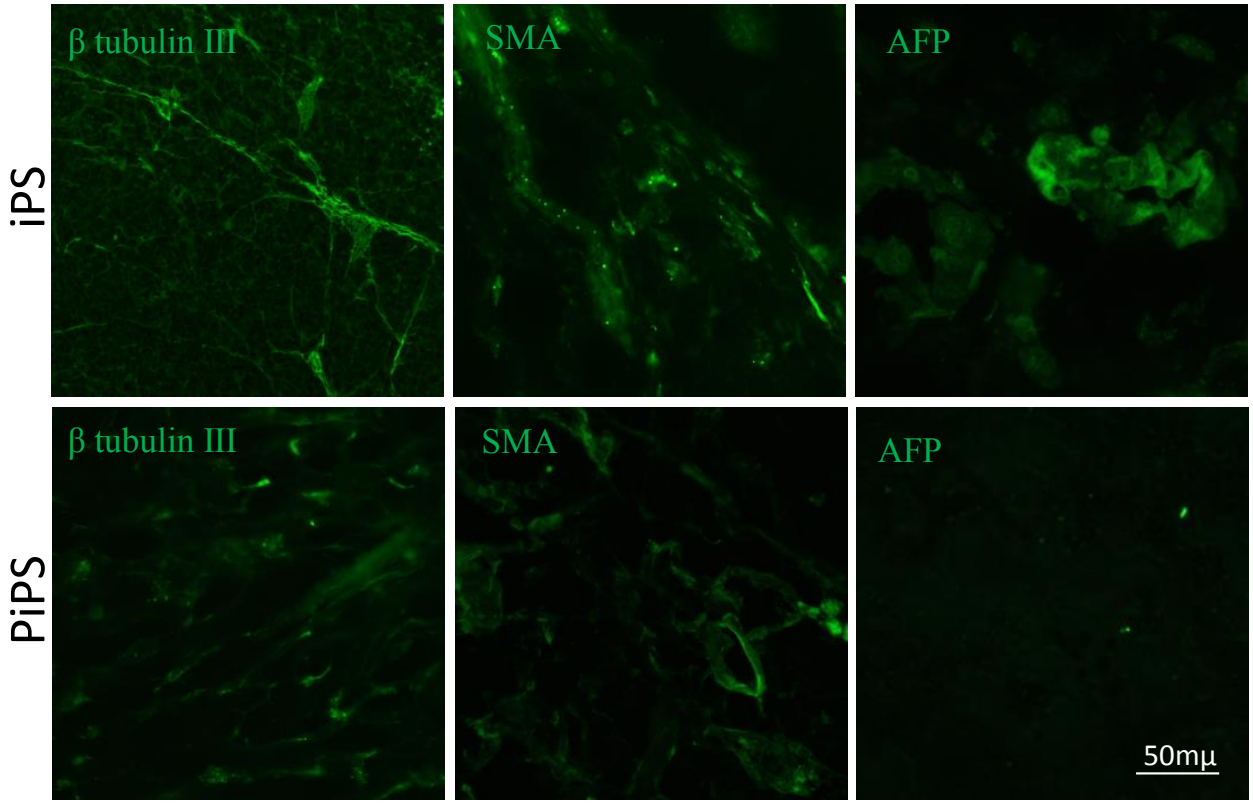

Online Figure II. Immunofluorescent staining for markers specific to the three germ layers. iPS or PiPS cells were transplanted into SCID mice for 2 months. Indirect immunofluorescent staining for markers specific to the ectoderm (β tubulin III), mesoderm (SMA) and endoderm (AFP) did not reveal characteristic structures of the respective germ layer in the PiPS-derived sections as opposed to the iPS-derived sections.

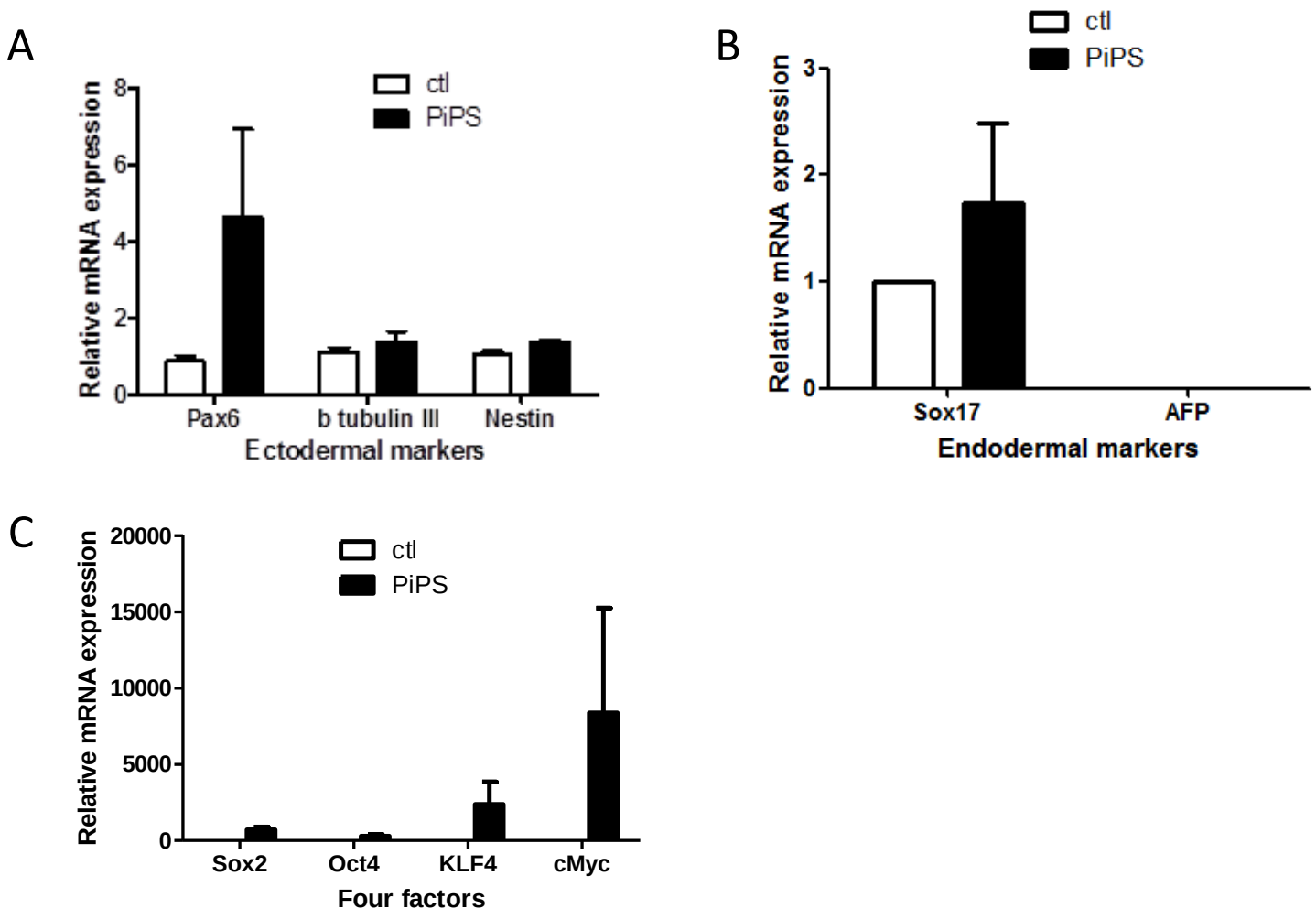

Online Figure III. Expression of ectodermal and endodermal markers in PiPS cells. Human fibroblasts were transfected with the 4 factors and maintained in reprogramming media for 4 days. No significant changes in the expression of ectodermal or endodermal markers were detected between PiPS and ctl cells. Notably, the expression of AFP was almost undetectable by Q-PCR (ct value >36) (means ± SEM of n=3).

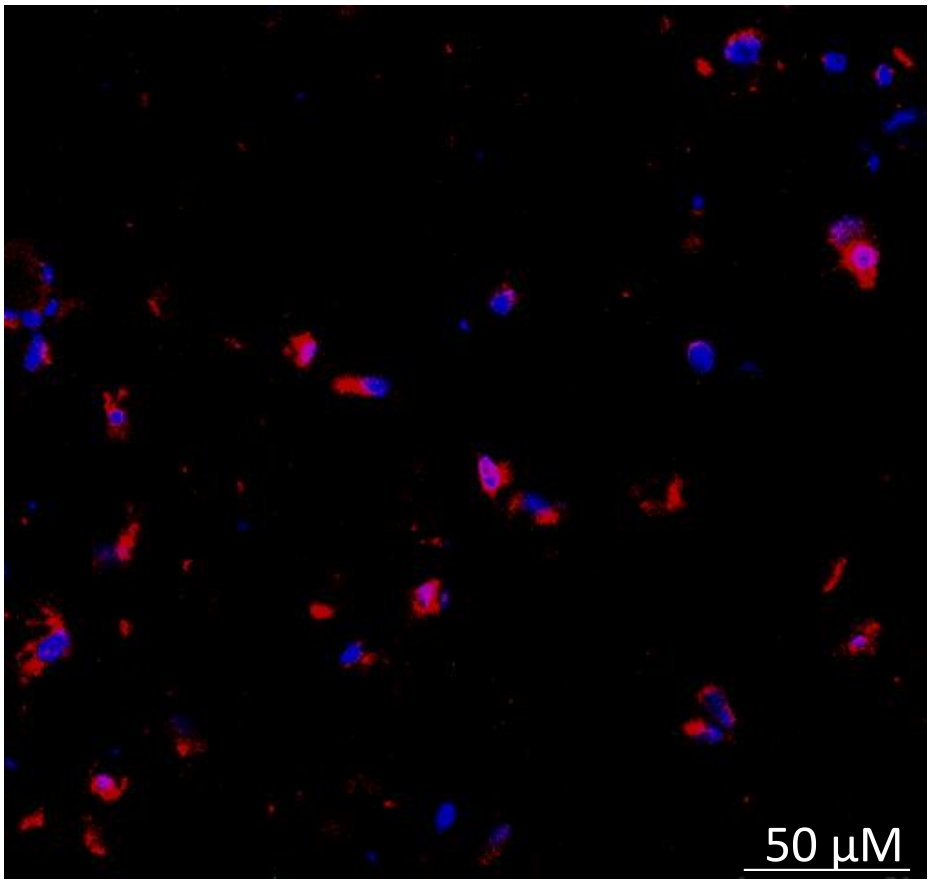

Online Figure IV. PiPS cells successfully incorporate within the tissues after subcutaneous transplantation in SCID mice. PiPS cells were labeled with Vybrant (red) and then subcutaneously injected into SCID mice. Fluorescent microscopy revealed that although PiPS did not proceed to teratoma formation, they successfully incorporated within the mouse tissues.

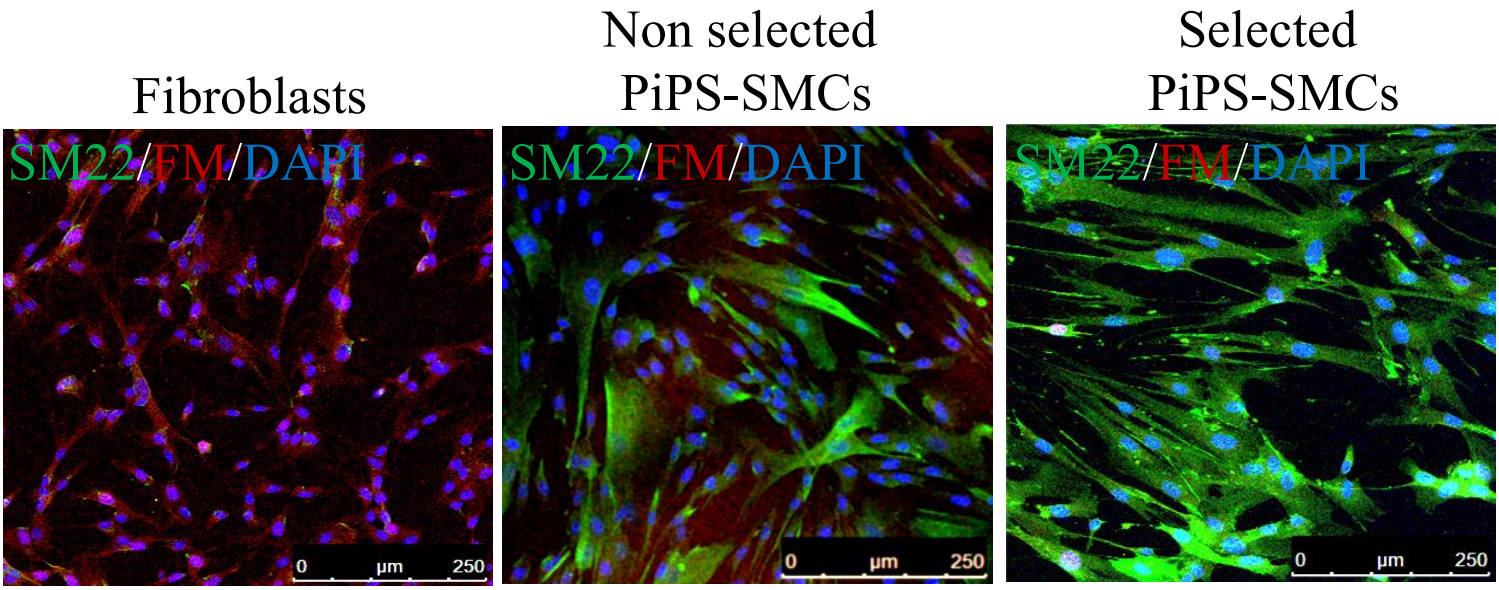

Online Figure V. PiPS cells differentiate to SMCs whereas the non reprogrammed cells remain fibroblastic. Human fibroblasts were reprogrammed for 4 days, a portion of which were selected with neomycin in order to obtain a pure population on PiPS cells. They were then seeded on Collagen IV and differentiated for 4 days. Indirect immunofluorescent staining for FM (Fibroblast Marker) and SM22 revealed that only the cells that have been successfully reprogrammed have differentiated towards SMCs whereas the non reprogrammed cells have remained in their fibroblastic state. Images were obtained by confocal microscopy.

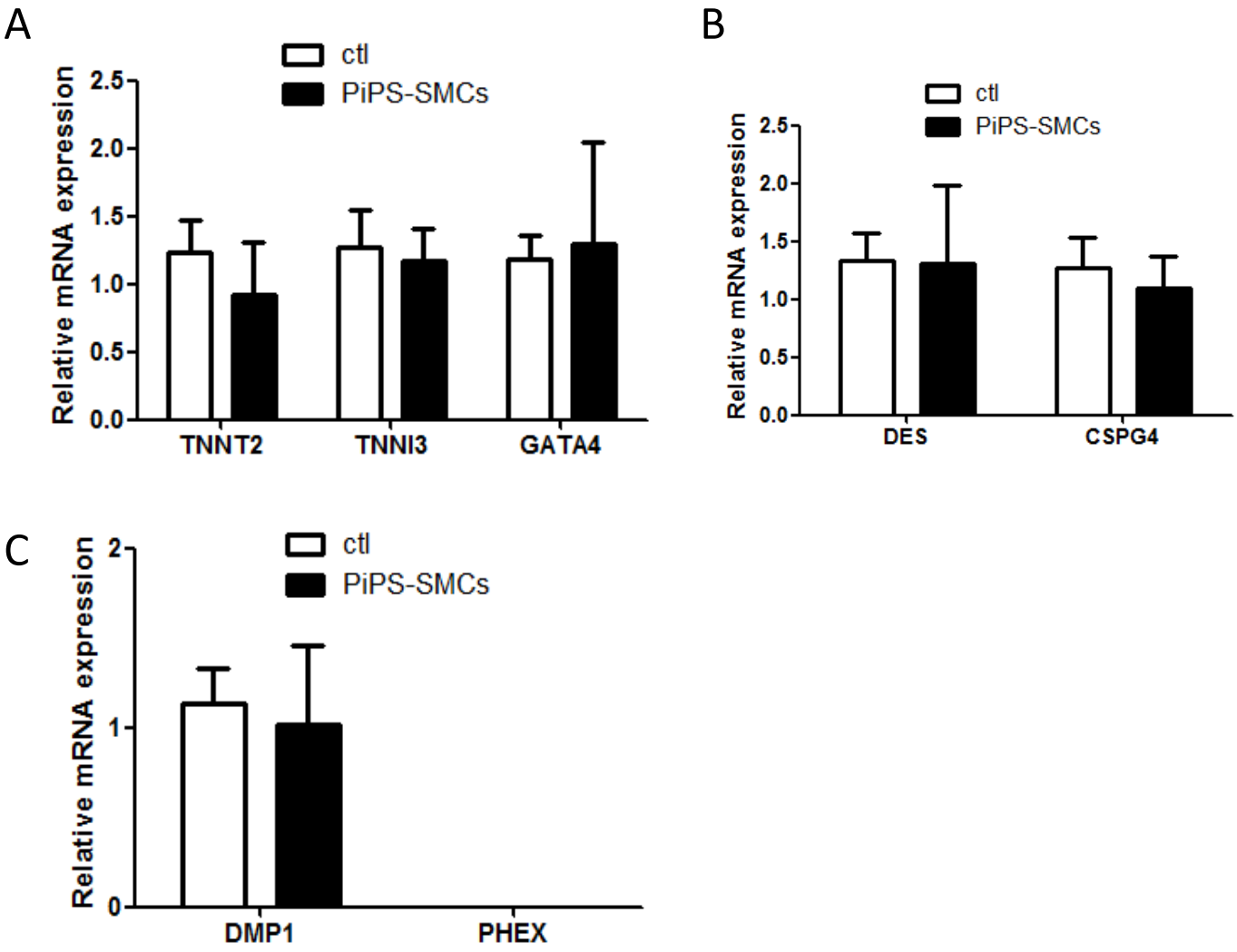

Online Figure VI. Examination of the expression of cardiomyocyte, pericyte and octeocyte markers in PiPS-SMCs. Human fibroblasts were reprogrammed and differentiated for 4D. They were then subjected to Q-PCR analysis where it was revealed that there was no significant upregulation of the cardiomyocyte (A), pericyte (B) or chondrocyte (C) markers between ctl and PiPS-SMCs. It should be noted that no expression of adipocyte markers was detected in either the ctl or PiPS-SMC samples (means ± SEM of n=3)

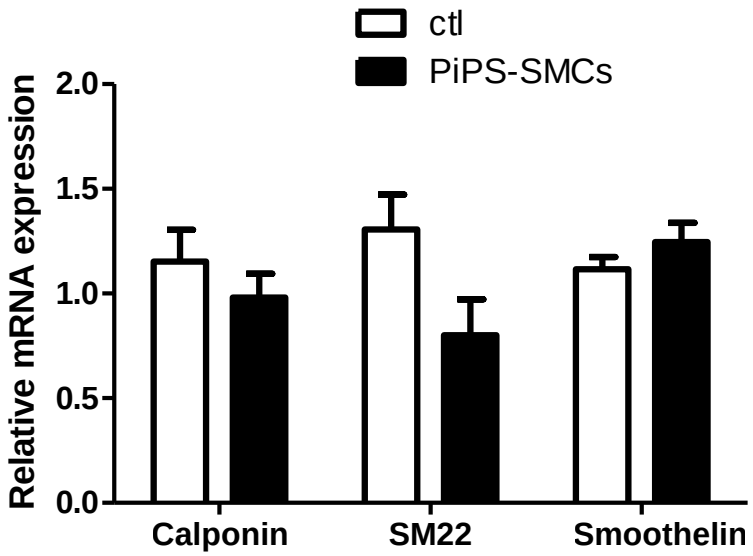

Online Figure VII. Differentiation potential of PiPS cells generated by skin fibroblasts. Human skin fibroblasts were nucleofected with ctl or OSKM vector and maintained in reprogramming media for 4 days. They were then seeded on a collagen IV substrate and maintained in DM for another 4 days. Q-PCR analysis revealed no significant differences in SMA, calponin and smoothelin (means ± SEM of n=3).

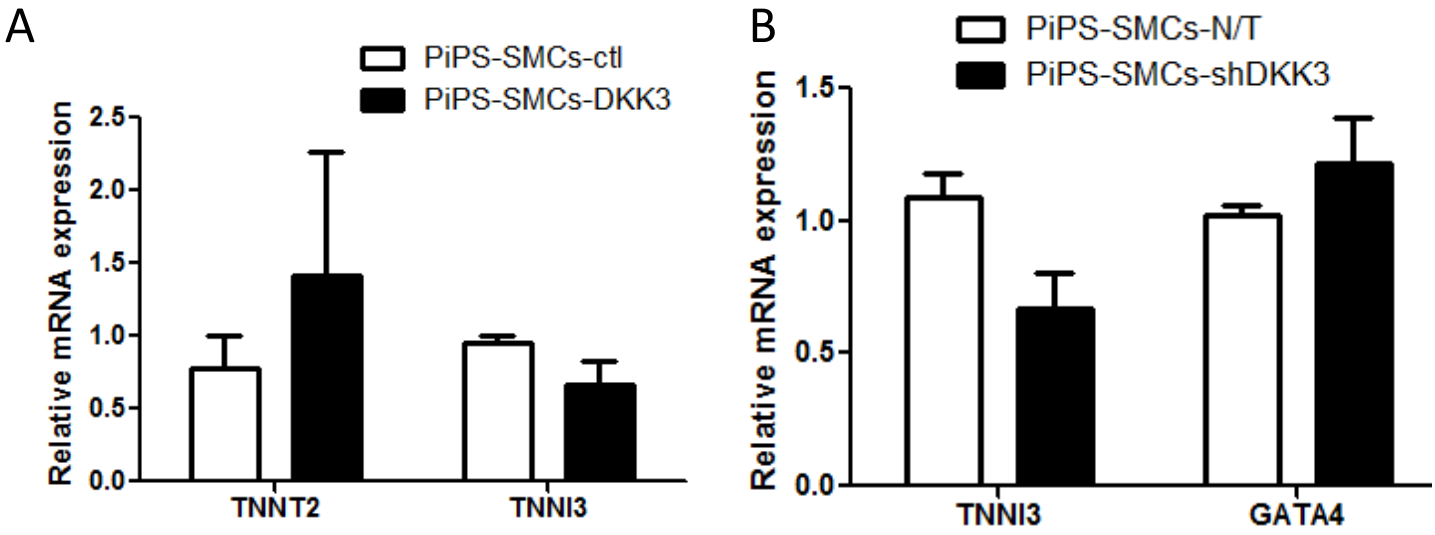

Online Figure VIII. DKK3 is specific for SMC differentiation within the cardiovascular lineages. DKK3 was overexpressed or knocked down in PiPS-SMCs. Total RNA was extracted and the samples were subjected to Q-PCR analysis. No significant differences were detected in the cardiomyocyte markers TNNT2, TNNI3 and GATA4 after supplementation or silencing of DKK3 (means ± SEM of n=3). No expression of endothelial markers was detected in either PiPS-SMCs or PiPS-SMC-DKK3 cells.

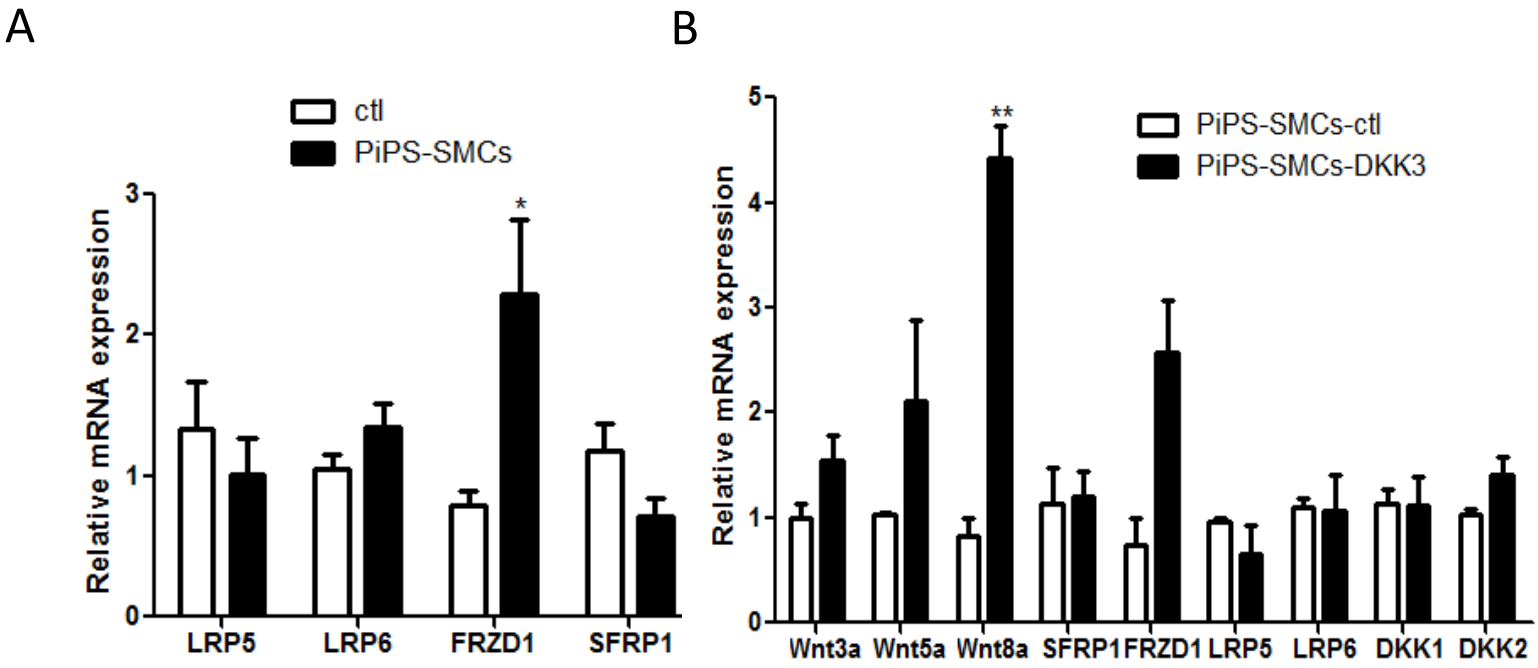

Online Figure IX. Expression of Wnt elements in PiPS-SMCs and PiPS-SMCs overexpressing DKK3. PiPS cells were differentiated for 4D after which total RNA was extracted and subjected to Q-PCR analysis. It was revealed that while there are no significant differences in the expression of LRP5, LRP6 and SFRP1, the Wnt receptor Frizzled 1 is upregulated between ctl and PiPS-SMCs (A). PiPS-SMCs were also forced to overexpress DKK3 after which the expression of a number of Wnt signaling components was detected by Q-PCR revealing no significant upregulations in the expression of the Wnt receptors but an upregulation in Wnts themselves (B) (means ± SEM of n=3, *$p<0.05$, **$p<0.01$)

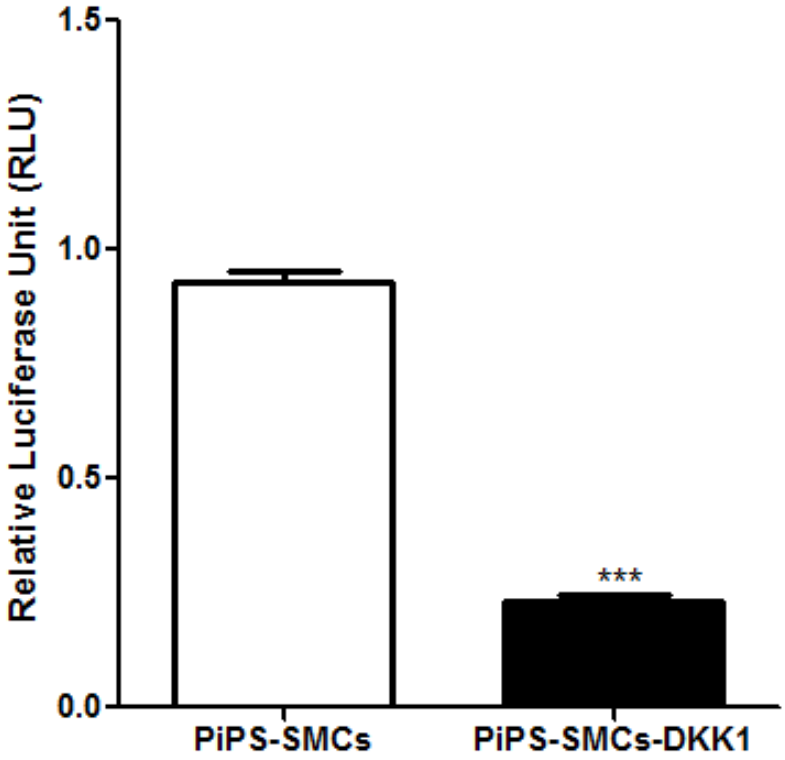

Online Figure X. DKK1 inhibits Wnt signaling in PiPS-SMCs. Luciferase assays for the activity of the TopFlash promoter were performed in PiPS-SMCs cells overexpressing DKK1. As shown, there is a dramatic downregulation of TopFlash activity upon DKK1 overexpression thus suggesting inhibition of Wnt signaling in PiPS-SMCs (means ± SEM of n=3, ***p<0.001)

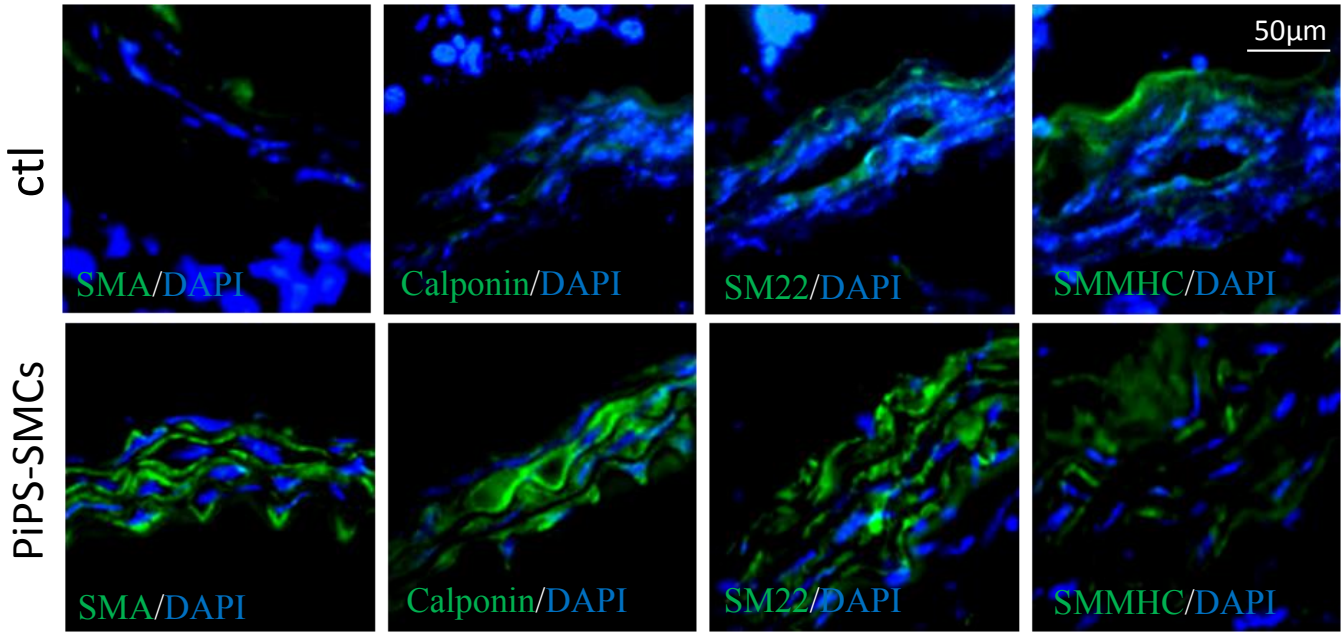

Online Figure XI. PiPS can successfully incorporate in *ex vivo* tissue engineered vessels. PiPS-SMC display SMC properties *ex vivo*. Ctl or PiPS cells selected for neomycin were seeded on a decellularised vessel scaffold and were differentiated towards SMCs for 5 days. Indirect Immunofluorescent staining for SMC markers revealed a characteristic SMC-like morphology and localization of PiPS-SMCs within the media of the vessels.

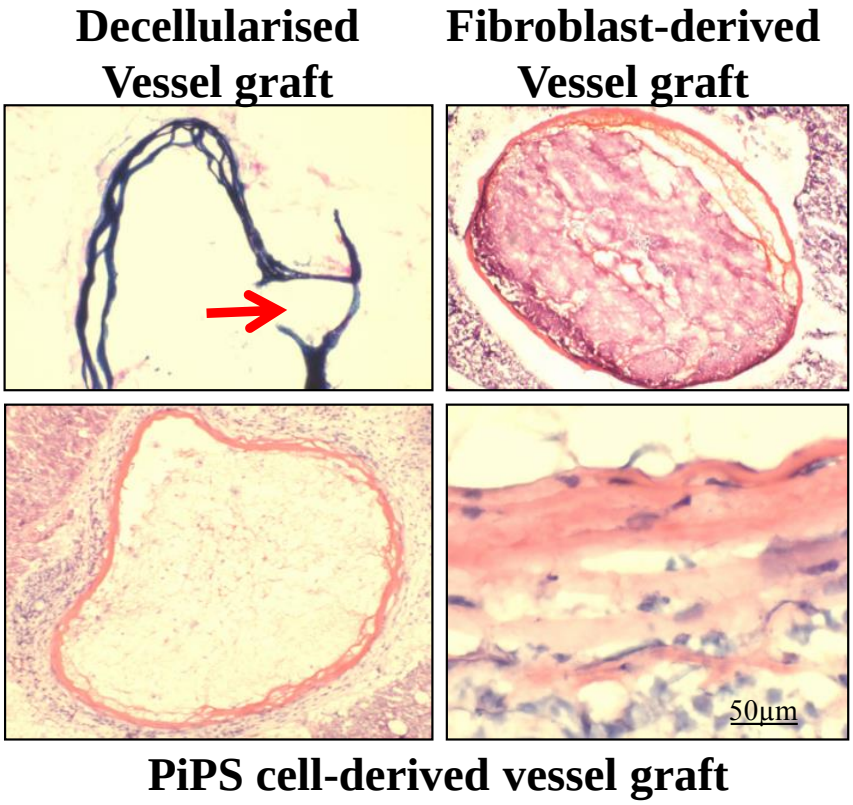

Online Figure XII. Double seeded PiPS cell-derived vessels form functional vessels after transplantation. Decellularised, fibroblast and PiPS-derived vessels were transplanted into SCID mice. It was revealed that while the fibroblast derived vessels were occluded via thrombus formation, the PiPS cell-derived vessels gave rise to patent vessels without rupturing or presenting with aneurism formation, which were comparable to native vessels. The decellularised vessels showed early wall dissection and ruptured early after transplantation.

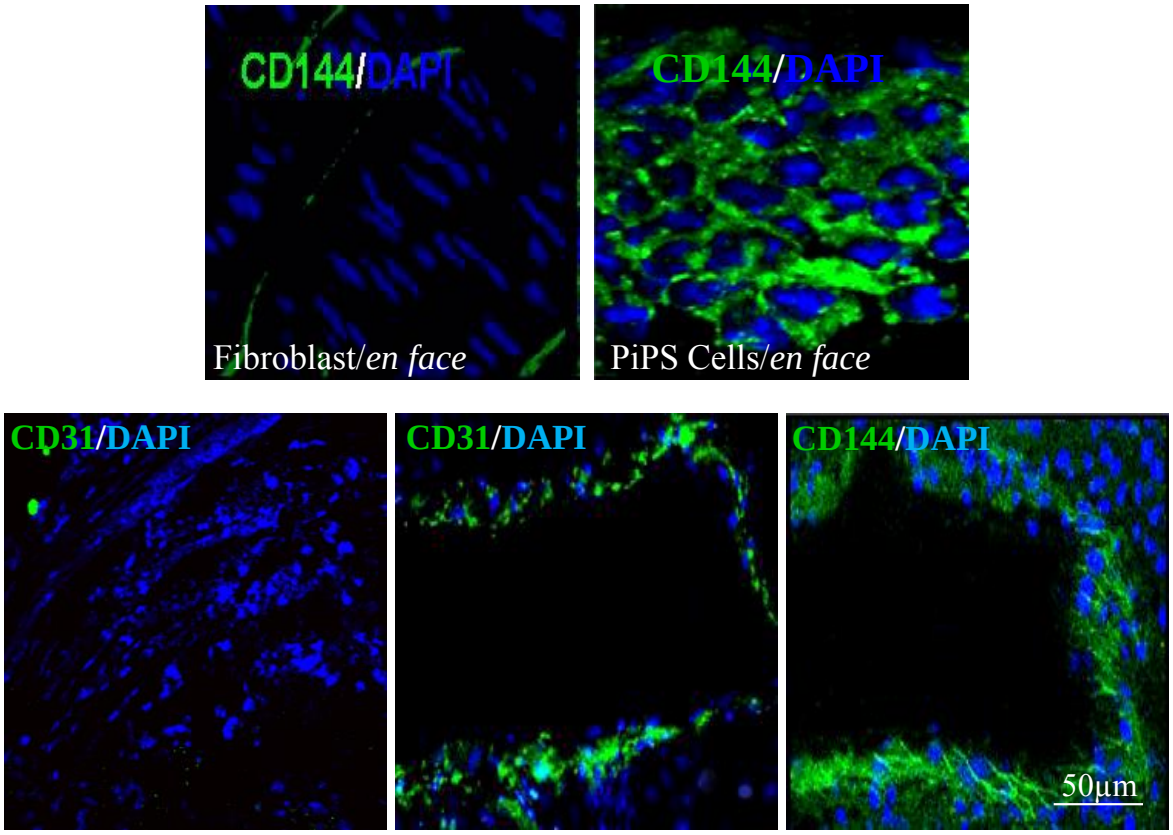

Online Figure XIII. Examination of post transplantation tissue engineered vessels. The tissue-engineered vessels were harvested 24 hours after grafting. The vessel segments were processed for *en face* preparation (upper panel) or cross section (lower panel) after which indirect immunofluorescent staining was performed for anti-human CD31 or CD144. The fibroblast seeded vessels developed with occlusion and wall adherent thrombus formation within the first 24 hours and stained negative for the above endothelial markers.

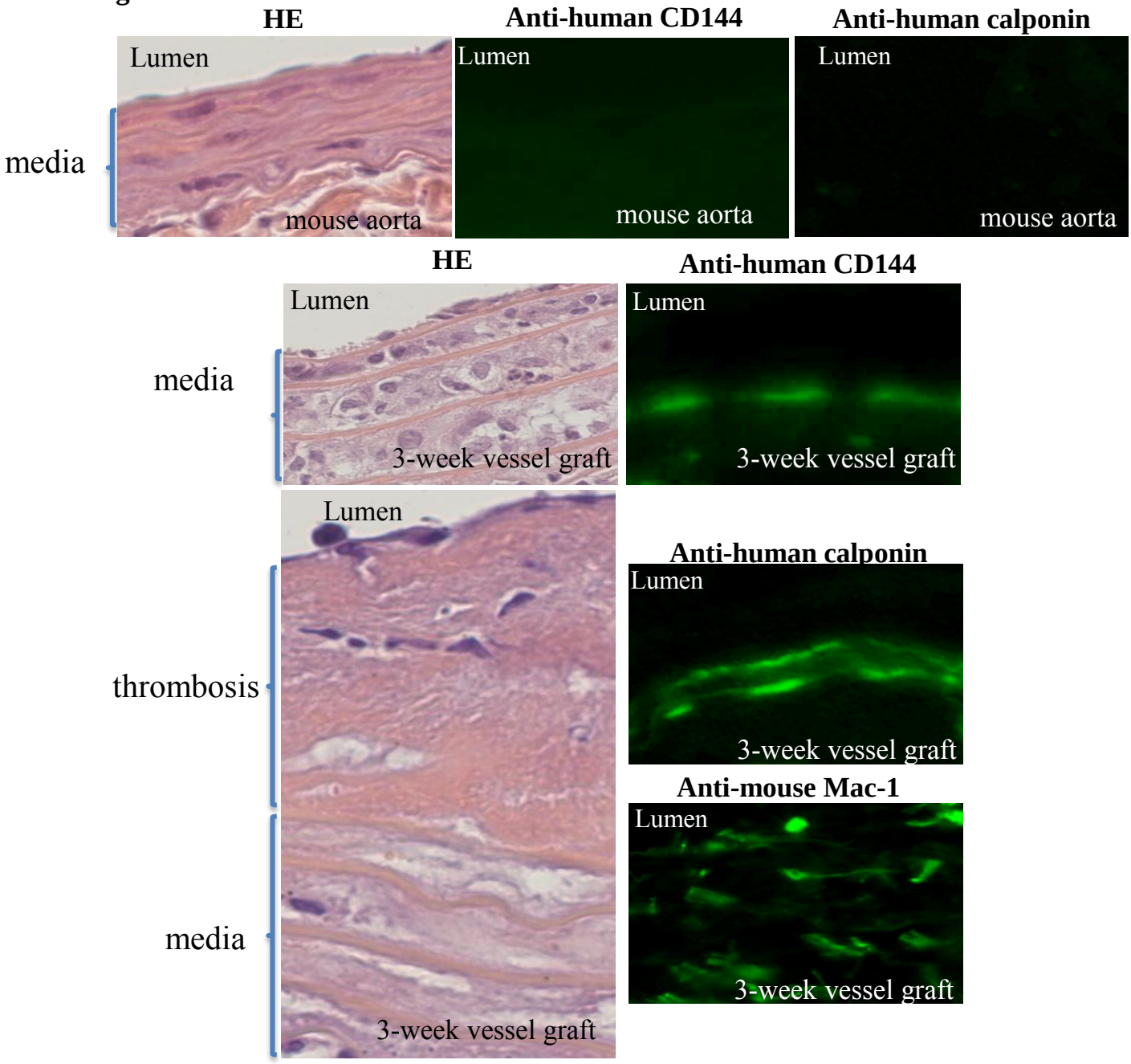

Positive cells Field (40x)	**Engineered-vessel graft (3 weeks)**	**Engineered-vessel before grafting**
calponin	22±11*	72±9
CD144	5±6*	20±8
Mac-1	71±11*	0

Online Figure XIV. The tissue-engineered vessels were harvested 3 weeks after grafting. The vessel segments were processed for HE section (left panel) or indirect immunofluorescent staining (right panel) for human CD144 and calponin or mouse Mac-1. The table below shows the data of means±SEM (n=6), *significant difference from tissue-engineered vessels before grafting, $p<0.05$. Original magnification x400.

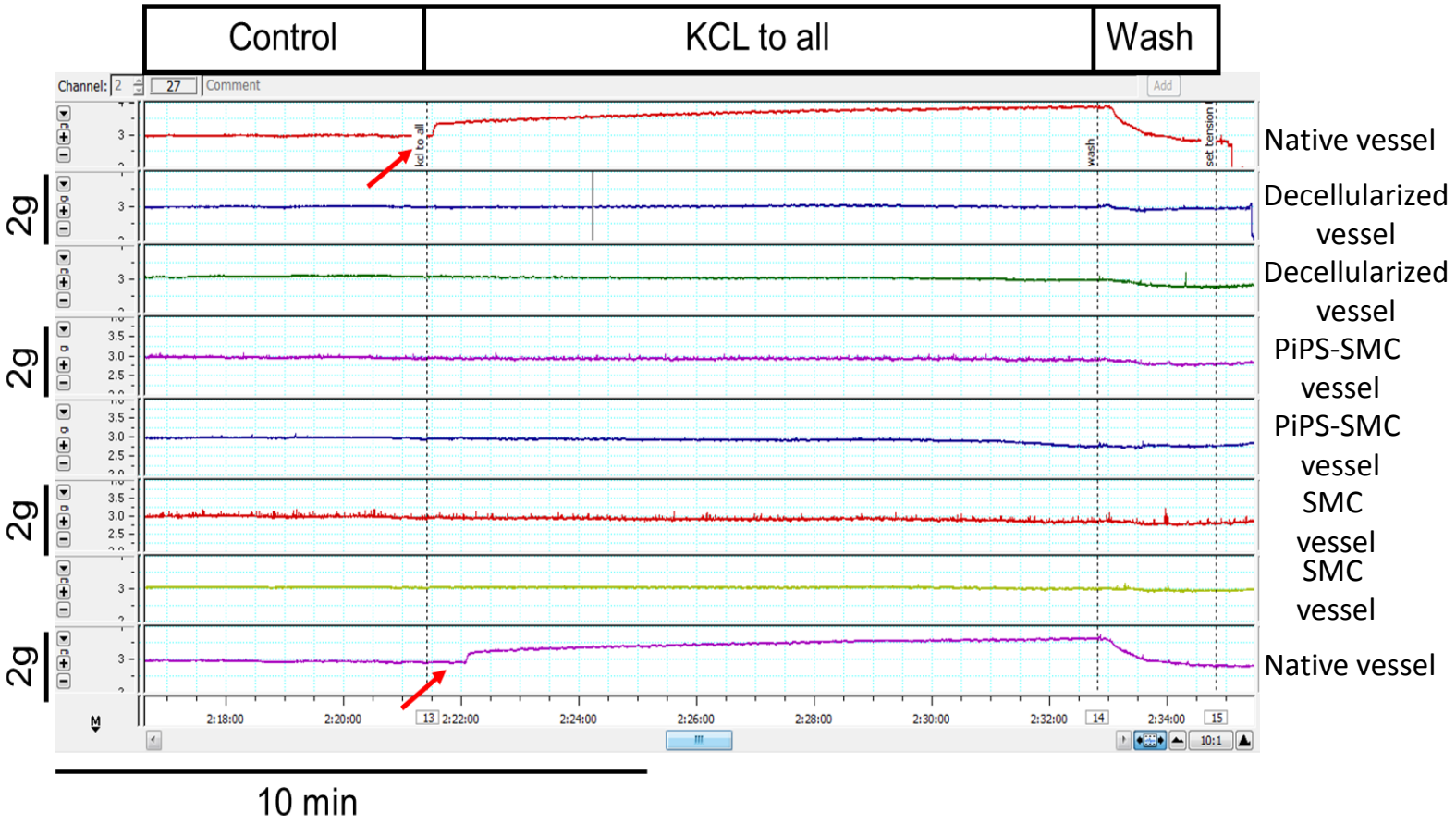

Online Figure XV. Contractility assay of native mouse vessels, SMC-derived and PiPS-SMC-derived tissue engineered vessels for KCl. 3 mm segments of the vessels were suspended in an organ bath containing Krebs buffer solution for isometric tension measurements. Resting tension was set to 3g and KCl (60mML) was added after a stabilization period of approximately 30 – 60 minutes. As expected, KCl induced a strong increase in tension in native mouse vessels but no response was observed in the SMC-derived and PiPS-SMC-derived vessels. Indicated with a red arrow is the response of the vessel to KCl stimulation.

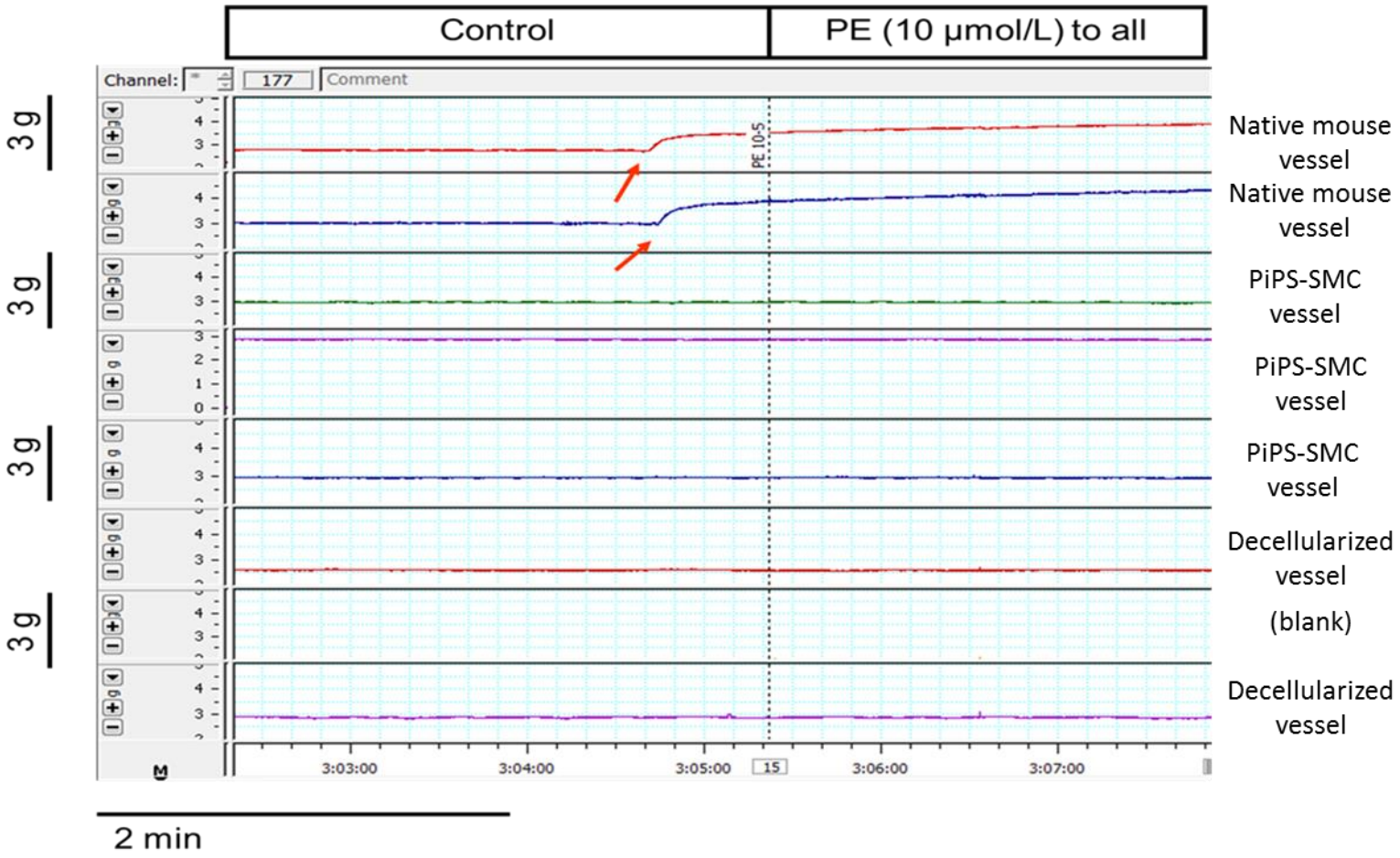

Online Figure XVI. Contractility assay of native mouse vessels, SMC-derived and PiPS-SMC derived tissue engineered vessels for phenylephrine. As described in Online Figure XV, isometric tension measurements of an independent experiment were performed in 3mm vessels at physiological conditions. Resting tension was set to 3g and phenylephrine (PE) (10µM) was added after a stabilization period of approximately 30 – 60 minutes. Similarly, as expected, PE induced a strong increase in tension in native mouse vessels but no response was observed in the SMC-derived and PiPS-SMC-derived vessels. Please note that no vessel was included in channel 7. Indicated with a red arrow is the response of the vessel to KCl stimulation.

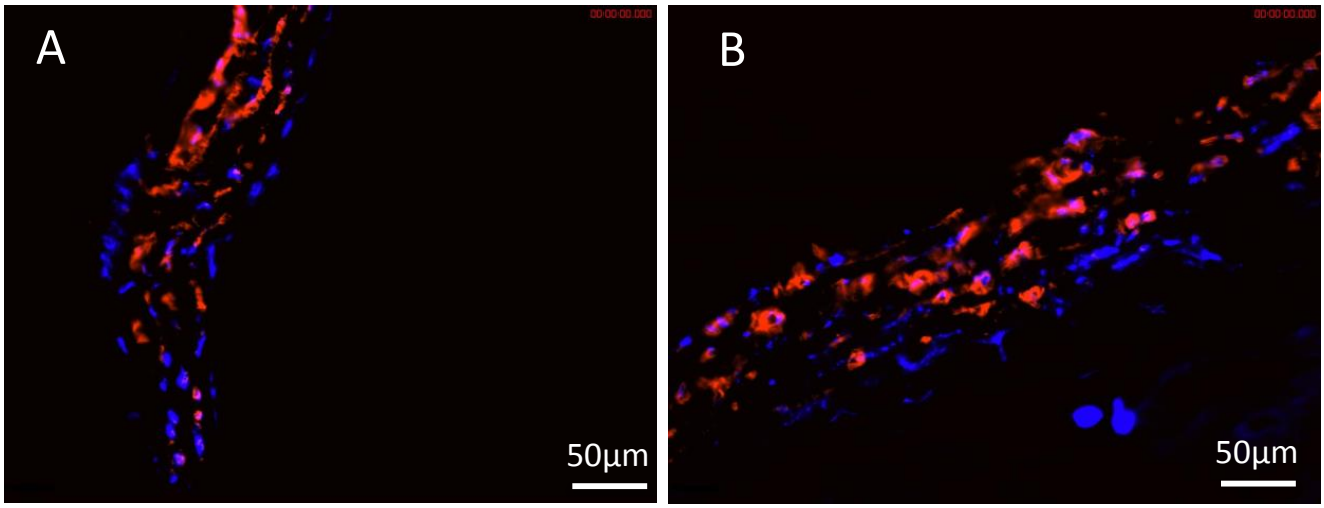

Online Figure XVII. PiPS cell-derived (A) and SMC-derived tissue engineered vessels (B) after tension bath contractility assay. The vessels were fixed and subjected to immunofluorescent staining for SMA after they were subjected to a tension bath contractility assay. The results revealed that although the cells present within the scaffolds are positive for SMA, they appear to have adopted a round morphology indicating successful contraction of the cells within the scaffold. DAPI was used as counterstaining of the nucleus.

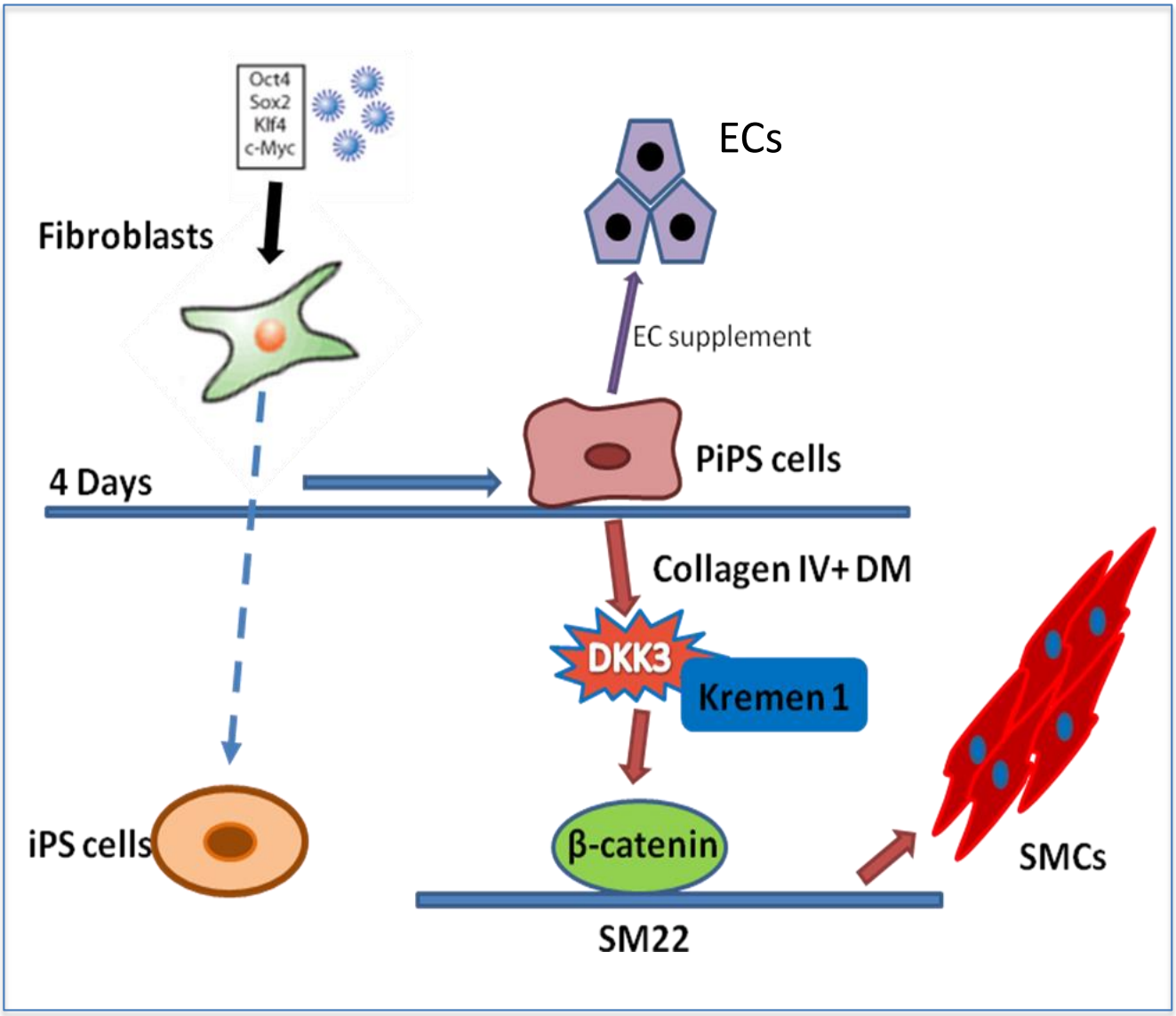

Online Figure XVIII. Schematic representation of the generation of PiPS cells as well as the mechanism by which DKK3 governs PiPS cell differentiation towards SMCs. PiPS cells can differentiate into SMCs via a DKK3-Wnt signalling pathway where DKK3 can regulate the transcriptional activation of SM22 through binding with Kremen 1, Wnt activation, and β-catenin translocation.

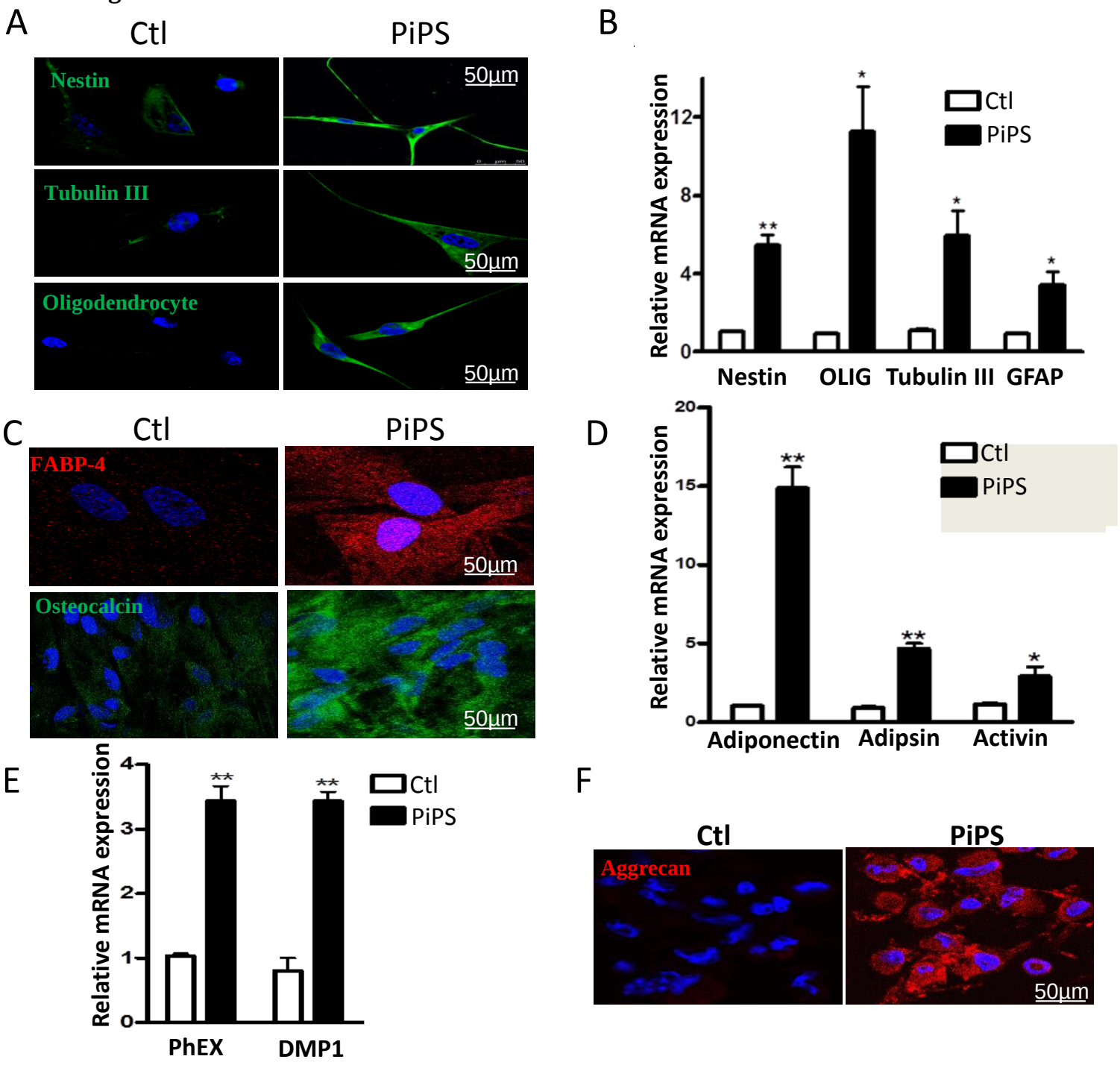

Online Figure XIX. PiPS cells can differentiate into neural cells, adipocytes, osteocytes and chondrocytes. PiPS or ctl cells were seeded in defined media to initiate neuronal cell differentiation for 7 days and stained with nestin, tubulin III, and oligodendrocyte markers (A). Q-PCR confirmed the expression of these genes at mRNA levels (B). PiPS cells differentiated into adipocytes, when cultured in adipocyte differentiation media for 10 days, as staining with FABP-4 indicates (C, upper panel). Q-PCR for adiponectin, adipsin, and activin (D). PiPS cells differentiated into osteocytes, when cultured with osteocyte media for 14 days and stained positive for osteocalcin (C, lower panel). Q-PCR assays with PHEX and DMP1, osteocyte markers, is shown (E) (means ± SEM. (n=3), *p<0.05, **p<0.01). PiPS cells showed expression for aggrecan (F) when they were cultured under chondrocyte differentiation defined conditions for 14 days.

Online Supplemental Tables

Online Table I: Primer sequences

Calponin	5'>TTGAGGCCAACGACCTGTTTGAGA<3' 5'>TCGAATTTCCGCTCCTGCTTCTCT<3'
SM22	5'>TTGAAGGCAAAGACATGGCAGCAG<3' 5'>TCCACGGTAGTGCCCATCATTCTT<3'
SMMHC	5'>AGAAGCCAGGGAGAAGGAAACCAA<3' 5'>TGGAGCTGACCAGGTCTTCCATTT<3'
SRF	5'>TGAGTGCCACTGGCTTTGAAGAGA<3' 5'>AGAGGTGCTAGGTGCTGTTTGGAT<3'
Myocardin	5'>TTGAAAGCGGAGAAATGCCAGCAG<3' 5'>ACTGTCGGTGGCATAGGGATCAAA<3'
DKK3	5'>AGGTTGAGGAACTGATGGAGGACA<3' 5'>ACCTTCGTGTCTGTGTTGGTCTCA<3'
β-catenin	5'>TGCAGTTCGCCTTCACTATGGACT<3' 5'>GATTTGCGGGACAAAGGGCAAGAT<3'
Axin2	5'>ACAACAGCATTGTCTCCAAGCAGC<3' 5'>GCGCCTGGTCAAACATGATGGAAT<3'
TCF1	5'>AATAGGGCGGAATGCATCCAGAGA<3' 5'>TTGGCAAACCAGTTGTAGACACGC<3'
18s	5'>CCAGAGCGAAAGCATTTGCCAAGA<3' 5'>TCGGCATCGTTTATGGTCGGAACT<3'
PHEX	5'>ACAACTTTGCTGCCTCAATGGGAC<3' 5'>TCGTTCCTGCATCCATCCACTCAT<3'
DMP1	5'>TGGAGATGACACCTTTGGTGACGA<3' 5'>TGGTGGTATCTTGGGCACTGTCTT<3'
ADIPOQ	5'>ATCCAAGGCAGGAAAGGAGAACCT<3' 5'>TGGTAAAGCGAATGGGCATGTTGG<3'
Adipsin	5'>TGATGTGCGCGGAGAGCAAT<3' 5'>TAGATCCCGGGCTTCTTGCGGTT<3'
ACVR1C	5'>TGGTTTACTGGGAAATAGCCCGGA<3' 5'>CACAACTTTGCCACTGGTTTGGGA<3'
NESTIN	5'>ACAGCCATAGAGGGCAAAGTGGTA<3' 5'>AAGGAACCTGGGAGTCCTGGATTT<3'
GFAP	5'>AGATTCGAGAAACCAGCCTGGACA<3' 5'>TTGTGCTCCTGCTTGGACTCCTTA<3'
TUBULIN III	5'>ATCAGCAAGGTGCGTGAGGAGTAT<3' 5'>TCGTTGTCGATGCAGTAGGTCTCA<3'
OLIGODENDROCYTE	5'>AAGATCAACAGCCGCGAGCGGAA<3' 5'>AGCGTGGCTATCTTGGAGAGCTT<3'
SM22 promoter mutation primers	5'>GGAATTGCAGTTCCCAGTAGGGCC<3' 5'>CCCTCCAGCAACAGCATTAATTCA<3'
Pax6	5'>GCGGAAGCTGCAAAGAAATAG<3' 5'>GGGCAAACACATCTGGATAATG<3'
AFP	5'> GCTGACCTGGCTACCATATTT<3' 5'> TGTTCATCTCCAGTGGGTTTC<3'
SOX17	5'> TTTCATGGTGTGGGCTAAGG<3' 5'> CCCAGCATCTTGCTCAACT<3'
Wnt3A	5'>GACTTCCTCAAGGACAAGTACG<3' 5'> GGCACCTTGAAGTAGGTGTAG<3'
WNT5A	5'>GGTGGTCGCTAGGTATGAATAA 5'>TCTTCTGTCCTTGAGAAAGTCC

Wnt8a	5'> CAGTGAGAGCCACCATGAAA<3' 5'> CCTGGTCATACTTGGCCTTTAG<3'
TNNI3	5'> GACAAGGTGGATGAAGAGAGATAC<3' 5'> CTTGCCTCGAAGGTCAAAGA<3'
TNNT2	5'> GGAGAGAGAGTGGACTTTGATG<3' 5'> CCTCCTCTTTCTTCCTGTTCTC<3'
GATA4	5'> GAAGGCAGAGAGTGTGTCAA<3' 5'> GCCGTTCATCTTGTGGTAGA<3'
DES	5'> ACACCAGATCCAGTCCTACA<3' 5'> AAATCGGTCCTCCAATTCCC<3'
CSPG4	5'> GACACAGGACAAGACCACTATG<3' 5'> TGGCGGGTAGCAACAAAT<3'
LRP5	5'>CCAGTACCCGCTGCAATAA<3' 5'>ATGACCGTGGTTTCGATCTC
LRP6	5'>GACCATCAGCAGAGCCTTTAT<3' 5'>GTTCTTCCCAAGCCAGTCTAC<3'
FZD1	5'>AAGACCGAGTGGTGTGTAATG<3' 5'>TGGCCATGCTGAAGAAGTAG<3'
SFRP1	5'>GCTTGTGCTGTACCTGAAGA<3' 5'>TCTTGTCCCACTTGTGGATG<3'
DKK1	5'>AGCACCTTGGATGGGTATTC<3' 5'>CTGATGACCGGAGACAAACA<3'
DKK2	5'>CCAGTACCCGCTGCAATAA<3' 5'>ATGACCGTGGTTTCGATCTC<3'

Online Table II: Microarray Analysis

Biological functions overrepresented in each cluster as determined using the DAVID software (Benjamini corrected P< 0.05).

Module	Category	Term	Count	Pvalue	Benjamini
1	GOTERM_BP_FAT	GO:0000279~M phase	41	3.74E-10	7.63E-07
1	GOTERM_BP_FAT	GO:0022403~cell cycle phase	45	4.60E-09	4.70E-06
1	GOTERM_BP_FAT	GO:0022402~cell cycle process	51	8.85E-08	6.02E-05
1	GOTERM_BP_FAT	GO:0006259~DNA metabolic process	45	2.29E-07	9.37E-05
1	GOTERM_BP_FAT	GO:0051321~meiotic cell cycle	16	1.95E-07	9.98E-05
1	GOTERM_BP_FAT	GO:0051327~M phase of meiotic cell cycle	15	7.85E-07	0.000266997
1	GOTERM_BP_FAT	GO:0007126~meiosis	15	7.85E-07	0.000266997
1	GOTERM_BP_FAT	GO:0007049~cell cycle	60	1.17E-06	0.00034004
1	GOTERM_BP_FAT	GO:0006260~DNA replication	24	2.45E-06	0.000626111
1	GOTERM_CC_FAT	GO:0000793~condensed chromosome	18	1.02E-05	0.001816337
1	GOTERM_CC_FAT	GO:0005694~chromosome	37	8.37E-06	0.002982852
1	GOTERM_CC_FAT	GO:0000228~nuclear chromosome	19	2.62E-05	0.003114093
1	GOTERM_BP_FAT	GO:0007067~mitosis	26	2.05E-05	0.00463278
1	GOTERM_BP_FAT	GO:0000280~nuclear division	26	2.05E-05	0.00463278
1	GOTERM_CC_FAT	GO:0044427~chromosomal part	31	6.75E-05	0.006003042
1	GOTERM_BP_FAT	GO:0000087~M phase of mitotic cell cycle	26	2.95E-05	0.006009755
1	GOTERM_BP_FAT	GO:0048285~organelle fission	26	4.20E-05	0.007129503
1	GOTERM_BP_FAT	GO:0048609~reproductive process in a multicellular organism	27	3.88E-05	0.007175452
1	GOTERM_BP_FAT	GO:0032504~multicellular organism reproduction	27	3.88E-05	0.007175452
1	GOTERM_BP_FAT	GO:0000278~mitotic cell cycle	35	5.78E-05	0.009039376
1	GOTERM_BP_FAT	GO:0019318~hexose metabolic	19	6.65E-05	0.009651951

		process			
1	GOTERM_BP_FAT	GO:0007498~mesoderm development	9	0.000104298	0.013223547
1	GOTERM_BP_FAT	GO:0006006~glucose metabolic process	16	0.000102831	0.013901919
1	GOTERM_BP_FAT	GO:0042698~ovulation cycle	9	0.000135628	0.015269503
1	GOTERM_BP_FAT	GO:0006974~response to DNA damage stimulus	32	0.000128344	0.015299105
1	SP_PIR_KEYWORDS	gluconeogenesis	6	4.16E-05	0.016098539
1	GOTERM_BP_FAT	GO:0005996~monosaccharide metabolic process	20	0.000151042	0.016103222
1	SP_PIR_KEYWORDS	glycolysis	9	0.000115544	0.022280473
1	GOTERM_BP_FAT	GO:0006096~glycolysis	9	0.00022167	0.022380809
1	GOTERM_BP_FAT	GO:0007059~chromosome segregation	13	0.000235582	0.022649773
1	GOTERM_BP_FAT	GO:0000226~microtubule cytoskeleton organization	16	0.000299719	0.027440058
1	GOTERM_BP_FAT	GO:0006310~DNA recombination	13	0.000357857	0.031277574

1	KEGG_PATHWAY	hsa00010:Glycolysis / Gluconeogenesis	10	0.000246141	0.032210564
1	GOTERM_BP_FAT	GO:0033554~cellular response to stress	39	0.000452321	0.036279445
1	GOTERM_BP_FAT	GO:0051301~cell division	27	0.00045025	0.037592608
1	GOTERM_BP_FAT	GO:0022602~ovulation cycle process	8	0.00055194	0.042433843
1	SP_PIR_KEYWORDS	dna replication	13	0.000333886	0.042483559
2	SP_PIR_KEYWORDS	transmembrane	117	4.61E-09	8.52E-07
2	SP_PIR_KEYWORDS	glycoprotein	88	4.02E-09	1.49E-06
2	UP_SEQ_FEATURE	glycosylation site:N-linked (GlcNAc...)	85	1.55E-09	1.74E-06
2	UP_SEQ_FEATURE	transmembrane region	117	3.23E-09	1.81E-06
2	SP_PIR_KEYWORDS	signal	71	2.15E-08	2.65E-06
2	SP_PIR_KEYWORDS	membrane	148	5.60E-08	5.18E-06

Supplemental References

1. Margariti A, Winkler B, Karamariti E, Zampetaki A, Tsai TN, Baban D, Ragoussis J, Huang Y, Han JD, Zeng L, Hu Y, Xu Q. Direct reprogramming of fibroblasts into endothelial cells capable of angiogenesis and reendothelialization in tissue-engineered vessels. *Proc Natl Acad Sci U S A*. 2012
2. Margariti A, Winkler B, Karamariti E, Zampetaki A, Tsai TN, Baban D, Ragoussis J, Huang Y, Han JD, Zeng L, Hu Y, Xu Q. Direct reprogramming of fibroblasts into endothelial cells capable of angiogenesis and reendothelialization in tissue-engineered vessels. *Proceedings of the National Academy of Sciences of the United States of America*. 2012;109:13793-13798
3. Margariti A, Xiao Q, Zampetaki A, Zhang Z, Li H, Martin D, Hu Y, Zeng L, Xu Q. Splicing of hdac7 modulates the srf-myocardin complex during stem-cell differentiation towards smooth muscle cells. *J Cell Sci*. 2009;122:460-470
4. Margariti A, Zampetaki A, Xiao Q, Zhou B, Karamariti E, Martin D, Yin X, Mayr M, Li H, Zhang Z, De Falco E, Hu Y, Cockerill G, Xu Q, Zeng L. Histone deacetylase 7 controls endothelial cell growth through modulation of beta-catenin. *Circ Res*. 2010;106:1202-1211
5. Krupnik VE, Sharp JD, Jiang C, Robison K, Chickering TW, Amaravadi L, Brown DE, Guyot D, Mays G, Leiby K, Chang B, Duong T, Goodearl AD, Gearing DP, Sokol SY, McCarthy SA. Functional and structural diversity of the human dickkopf gene family. *Gene*. 1999;238:301-313
6. Dietrich H, Hu Y, Zou Y, Dirnhofer S, Kleindienst R, Wick G, Xu Q. Mouse model of transplant arteriosclerosis: Role of intercellular adhesion molecule-1. *Arterioscler Thromb Vasc Biol*. 2000;20:343-352
7. Murdoch CE, Alom-Ruiz SP, Wang M, Zhang M, Walker S, Yu B, Brewer A, Shah AM. Role of endothelial nox2 nadph oxidase in angiotensin ii-induced hypertension and vasomotor dysfunction. *Basic research in cardiology*. 2011;106:527-538